Rivista Italiana di Paleontologia e Stratigrafia	volume 120	no. 3	pp. 317-335	December 2014

TECTONIC AND CLIMATIC CONTROL ON DEPOSITION OF SEEP-CARBONATES: THE CASE OF MIDDLE-LATE MIOCENE SALSOMAGGIORE RIDGE (NORTHERN APENNINES, ITALY)

ANDREA ARTONI [1*], STEFANO CONTI [2], ELENA TURCO [1] & SILVIA IACCARINO [1]

Received: July 21, 2014; accepted: October 16, 2014

Key words: Northern Apennines, foredeep, middle-late Miocene, seep-carbonates, Mi5 cooling event, tectonics.

Abstract. Seep-carbonates are generally related to hydrocarbon seepage on continental margins. Modern cold seeps are abundant in actively deforming tectonic settings, suggesting that tectonics is one of the major controlling factor on fluid emissions. Hydrocarbon seepages are considered major geological sources of atmospheric methane, one of the most important green-house gases, and have also been related to climate changes. However, the interplay between tectonics and climate change in forcing seepage is not clearly understood. Miocene seep-carbonates, formed in a collisional setting such as that of the Salsomaggiore area of the Northern Apennines (Italy), provide an opportunity to assess accumulation and release of methane in response to tectonics and climate change along a convergent margin. The studied seep-carbonates are related to fluid emissions of various intensities coeval with tectonic pulses. New planktonic foraminiferal biostratigraphic data reveals that deposition of these seep-carbonates is late Serravallian-early Tortonian in age and partially coeval with the Miller's global cooling event Mi 5 (as used below). These seep-carbonates were deposited in two stages with different seepage modes. During the first stage, local tectonic pulses at the onset of the Mi5 event may have produced slow seepage, whereas during the second stage regional tectonics and more extreme climatic conditions (coolest peak of Mi5 event) may have resulted in a fast and more intense seepage as suggested by increasing occurrence of chaotic facies. In the Salsomaggiore Ridge, tectonics and the Mi5 cooling event actively concurred to the deposition of seep-carbonates in both stages.

Introduction

Studies of seep-carbonates related to hydrocarbon seepage, and in particular to methane-rich fluids, are of prominent interest because methane is one of the major green-house gases and its increase can cause atmospheric temperature rises (Kennett et al. 2003; Etiope et al. 2008; Etiope 2012). Seep-carbonates have been related to cold and hydrocarbon-rich fluid vents occurring at sea-floor (Judd & Hovland 2007; Suess 2014). In the vent's sites, specialized chemosynthetic biological communities develop (Campbell 2006; Han et al. 2008; Taviani 2014). When the venting fluids and specifically the methane-rich fluids react with O_2 dissolved in sea-water, the methane is oxidized, the newly formed CO_2 is released to the atmosphere and carbonates precipitate at sea floor (Jørgensen 1976; Sloan 1998). Microbially mediated oxidation of methane is recognized to be the prevailing biochemical reaction at vent sites: anaerobic oxidation of methane (AOM) of the literature (Suess 2010 and references therein). These carbonates have a typical geochemical signature because they are relatively depleted in ^{13}C isotope (Sloan 1998; Greinert et al. 2001; Campbell et al. 2002; Han et al. 2004).

Many different sources contribute to the fluxes of methane to and from the atmosphere (Kvenvolden & Lorenson 2001; Etiope 2012); the fluxes can be synchronous worldwide and extremely variable in rate and intensity over time (Nisbet 1990; Wuebbles & Hayhoe 2002). The present-day emissions of methane derived from geological sources (mud volcanoes, sediment instability, micro-seepage, marine seepage, geothermal fluxes) are rather underestimated. It is presumed that geologically sourced methane comes predominantly from gas hydrates stored in marine sediments (Hovland

1 * Corresponding author. Dipartimento di Fisica e Scienze della Terra, Università degli Studi di Parma, Parco Area delle Scienze 157/A, 43124 Parma, Italy. E-mail: andrea.artoni@unipr.it

2 Dipartimento di Scienze Chimiche e Geologiche, Università degli Studi di Modena e Reggio Emilia, Largo S. Eufemia 19, 41121 Modena, Italy.

et al. 1993; Kvenvolden & Rogers 2005; Etiope et al. 2008). According to global estimates, convergent margins may contain two-thirds of the global gas hydrate reservoir (Kastner 2001); however, these estimates should be carefully evaluated (Milkov 2004) especially with respect to long-term emissions (Bangs et al. 2011) and detailed global distributions (Suess 2010, 2014; Suess & Haeckel 2010).

On the basis of geochemical and paleontological proxy records, some of the climate changes that occurred during the Quaternary (Petit et al. 1999; Monnin et al. 2001; Kennett et al. 2003) and the Paleogene (thermal maximum/LPTM in Katz et al. 1999 and Dickens 2004) have been related to variations in methane concentration in the atmosphere (Dickens et al. 1995; Sluijs et al. 2007; Secord et al. 2010). Moreover, the Authors cited above and Teichert et al. (2003) suggested that the climatic changes controlled the occurrence of seep-carbonates related to methane emissions.

One of the primary sources for methane release into the atmosphere is currently understood to be the destabilization of gas hydrates, which are very sensitive to changes in pressure/temperature conditions (Sloan 1998; Suess 2011). Destabilization of gas hydrates is suggested to occur: 1) during the interglacial times when the temperature of intermediate water rises and global warming is amplified (the clathrate gun hypothesis of Kennett et al. 2000, 2003; Hill et al. 2006), or 2) during glacial times when sea level drops and hydrostatic pressure at sea floor decreases (Kvenvolden 1993; Fichler et al. 2005; Luyendyk et al. 2005).

However, tectonics is regarded as one of the major factor controlling the release of methane and destabilization of hydrate reservoirs, especially along convergent margins (Lallemand et al. 1992; Suess et al. 1998, 1999; von Rad et al. 2000; Obzhirov et al. 2004; Aiello 2005). Pressure changes due to variations in stress conditions can destabilize gas hydrates and trigger fluid migrations (Bohrmann et al. 1998; Sassen et al. 2001; Schwartz et al. 2003; Trèhu et al. 2004, 2006; Weinberger & Brown 2006; Fischer et al. 2013).

Seep-carbonates documenting the fluid expulsion enriched in methane have been identified in the Northern Apennines. These deposits, known as "*Lucina* limestones" (Ricci Lucchi & Vai 1994) and studied since long time (see Conti et al. 1993; Taviani 2001, 2014 for a historical review), occur in different tectonic sedimentary settings, from the foredeep to satellite basins (Conti et al. 2014). Some of these deposits have been related to tectonic activity, both local and regional, (Conti & Fontana 2005; Conti et al. 2007, 2010). However, other seep-carbonates located in the Apenninic foredeep seem to be associated with climatic changes. This is the case of seep-carbonates enclosed in the Miocene Vicchio Marls, whose deposition has been related to the global cooling event Mi3b (Fontana et al. 2013).

In the Salsomaggiore area (Northern Apennines, Italy; Fig. 1), seep-carbonates deposited during the late Serravallian have been related by Conti et al. (2007) to tectonic pulses. However, this time interval is characterized by the global cooling event Mi5 (Miller et al. 1991a, 1991b). Therefore, the aim of this paper is to investigate and discriminate the role of tectonics and climate change on the deposition of seep-carbonates in the Salsomaggiore Ridge (SR). In addition to an updated description of the sedimentological and geochemical characters of seep-carbonate facies, derived from and complementary to that of Conti et al. (2007), new biostratigraphic results based on planktonic foraminifera are here presented. The resulting updated stratigraphic scheme allows the identification of timing and mode of seep-carbonate deposition.

Geological setting of Northern Apennines and Salsomaggiore area

The Northern Apennines are a fold-and-thrust belt characterized by stacking of several structural units (Fig. 1). The complex structure of the orogenic belt is the result of convergence between the European and the African plates from the Cretaceous to the Recent. This process caused the progressive consumption of the Piedmont-Ligurian Ocean, a portion of the Mesozoic Tethys (Cavazza et al. 2004 and reference therein), and the inception of continental collision. Since Cretaceous to middle Eocene, the collisional processes were related to the eastward subducting European plate which created the Alpine orogenic wedge (Doglioni et al. 1998; Guegen et al. 1998). Since late Eocene-Oligocene, the west-dipping subduction and retreating/rolling-back of African/Adria plate dominated the collisional processes which created the Apenninic orogenic wedge, while the Alpine orogen was dismembered by back-arc extension creating the Balearic Sea (Malinverno & Ryan 1986; Royden et al. 1987; Patacca et al. 1990; Doglioni et al. 1998; Carminati & Doglioni 2012). During late Oligocene to Recent collisional phases, the internal and previously accreted oceanic units (Ligurian units) were thrusted over the western continental margin of Africa, together with epi-Ligurian wedge-top basins (Boccaletti et al. 1990; Amorosi et al. 1993; Conti & Gelmini 1994; Cibin et al. 2001). The fold-and-thrust belt and the associated foreland basin system of the Apennine orogenic wedge migrated eastward toward the foreland area, where metamorphic basement and a Mesozoic to Miocene sedimentary succession (Tuscan and Umbrian units, part of the Africa plate) form the lower structural

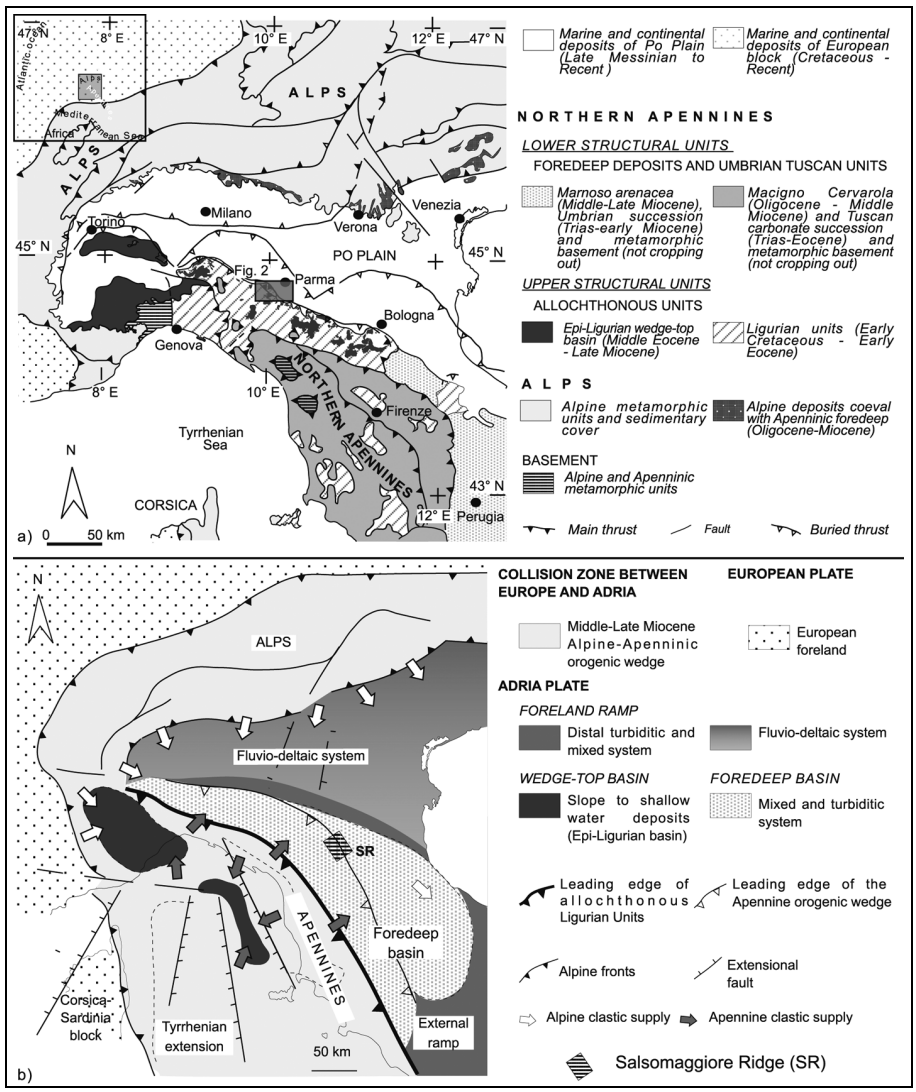

Fig. 1 - a) Location of the study area and geologic sketch map of the Northern Apennines. b) Paleogeographic map of the area of Salsomaggiore Ridge (SR) at the leading edge of the Northern Apennines orogenic wedge during the middle-late Miocene (modified after Mutti et al. 2002).

units of the Apennines (Doglioni et al. 1998; Guegen et al. 1998; Argnani & Ricci Lucchi 2001) (Fig. 1a).

During the Miocene, the foredeep depocenters and the allochthonous units migrated in response to the advancing orogenic leading edges. At the same time, the external foreland ramp was flexing and migrating eastward, while the foredeep depocenters were filled predominantly by turbidites (Ricci Lucchi 1975, 1986; Argnani & Ricci Lucchi 2001; Mutti et al. 2009) and mixed system deposits (*sensu* Mutti et al. 2002, 2003) derived from rivers and deltas mainly draining the Alps and, locally, the Apennines (Fig.1b).

The Salsomaggiore area

The Salsomaggiore Structure is a tectonic window where the middle-upper Miocene foredeep deposits (mainly Langhian-Serravallian in the lower structural units) crop out underneath the allochthonous units (upper structural units) (Artoni et al. 2004; Figs 1, 2). The folded Langhian-Serravallian foredeep deposits form the Salsomaggiore anticline (Salsomaggiore Ridge, SR from now), which is a fault-propagation anticline related to a fault buried beneath the Messinian to Recent deposits (Artoni et al. 2007, 2010) (Fig. 2b). The Langhian unit is made up of hemipelagic marls (Torrente Ghiara Formation) separated from the overlying Serravallian turbidites (Rio Gisolo Formation) by an onlap surface (Zanzucchi 2000; APAT-Regione Emilia Romagna 2000); this surface represents an unconformity referred to as U1 in the present work (Figs 2 and 3). The facies associations and distribution of the Serravallian foredeep deposits show that they originated by cohesive and/or turbulent mass flows. They can be ascribed to poorly efficient depositional lobes of mixed system type B (*sensu* Mutti et al. 2003) directly fed from a deltaic area; these lobes have proximal coarser-grained facies (Monte Predella Member) and more distal finer-grained facies (Varano dei Marchesi Member). On the south-western limb of the SR, close to Monte Predella (Fig. 2c), the Serravallian coarse-grained foredeep deposits are overlain by hemipelagic and prodeltaic marls (Case Gallo Formation of Zanzucchi 2000), which are about 50 m thick. According to Conti et al. (2007), these marls were eroded and then overlain by a chaotic unit,

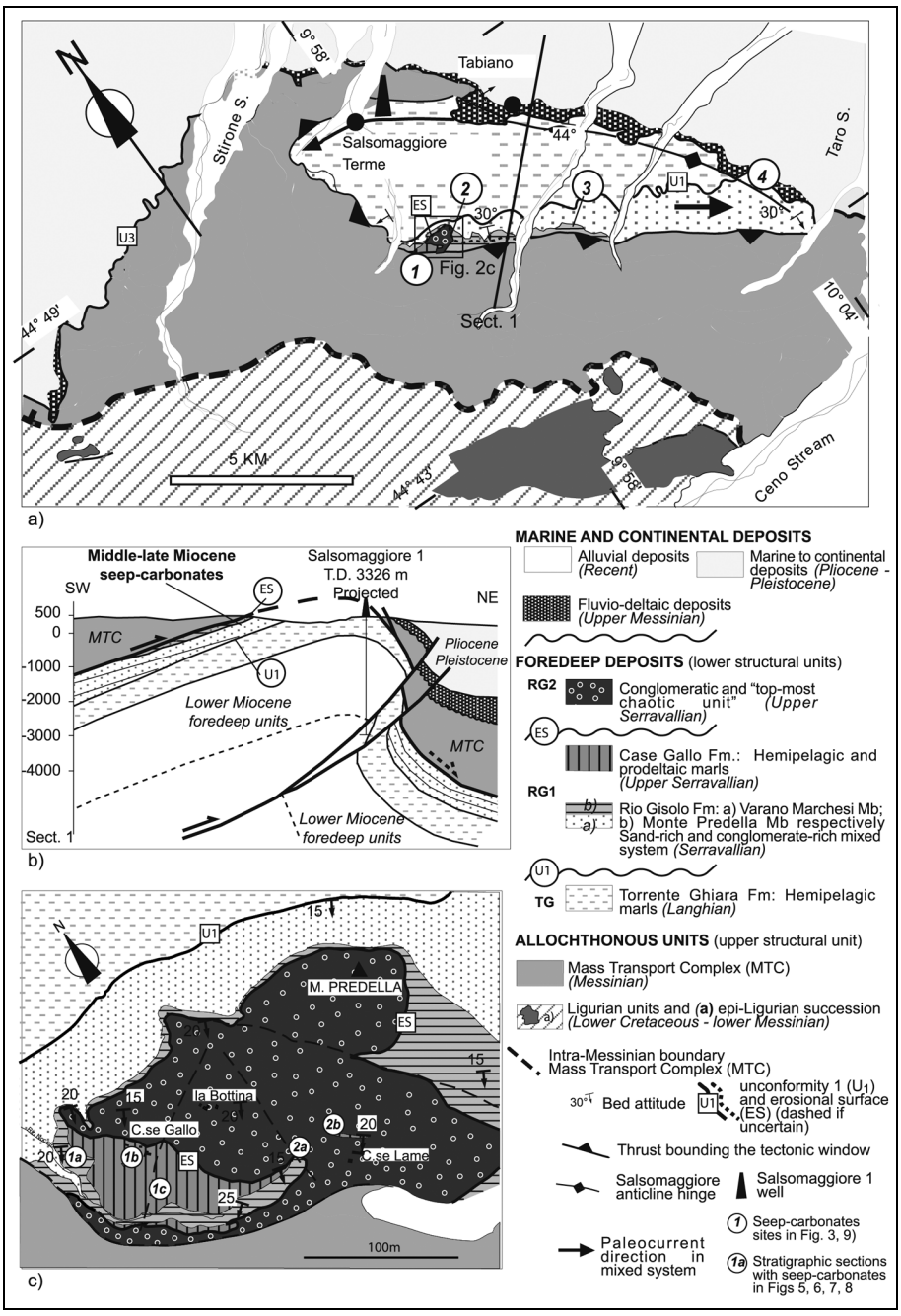

Fig. 2 - a) Geologic map of the Salsomaggiore Structure and locations of the four sites containing the seep-carbonates. b) Cross-section across the Salsomaggiore anticline (for location see a), a thrust-related anticline sealed by late Messinian to Recent deposits. c) Schematic geological map of a portion of the southern flank of the Salsomaggiore Ridge close to Monte Predella where the stratigraphic sections of sites 1 and 2 come from (see Figs 5-7); in this locality, the "topmost chaotic unit" with reworked seep-carbonates is well exposed and erodes down into the Case Gallo Formation (modified after Piola 2003).

maximum 10 m thick. This "topmost chaotic unit" consists of disorganized and immature ortho- and/or paraconglomerates and was included in the Monte Predella Member in previous works (Zanzucchi 2000; APAT-Regione Emilia Romagna 2000). The Middle Miocene stratigraphic succession is overthrust by the allochthonous units which are unconformably sealed by late Messinian to Recent fluvio-deltaic and alluvial deposits (Figs. 2a and 3) (Artoni et al. 2004, 2010).

The upper part of Rio Gisolo and the Case Gallo Formations (Figs 2, 3) includes irregular carbonate bodies and lenses with a typical macrofauna dominated by lucinid clams, known as "*Lucina* limestones" (Conti et al. 1993; Taviani 2001) and related to hydrocarbon seepage by Conti et al. (2007).

Material and methods

The SR seep-carbonates were studied by integrating previously published field mapping (Artoni et al. 2010), synthesis of sedimentological and geochemical analyses from Conti et al. (2007) and planktonic foraminiferal biostratigraphy.

Five composite stratigraphic sections crossing the seep-carbonates and their enclosing strata were measured at two sites on the southern limb of SR (sites 1 and 2 in Figs. 2a and 3). The entire thickness of the studied stratigraphic succession is about 50 m, while that of individual seep-carbonate unit is around 2-4 m. Seep-carbonates were also observed in other two sites (site 3 on the southern limb and site 4 on the northern limb of SR, Fig. 2a) but they were not useful for stratigraphic correlation.

Micropaleontological analysis of planktonic foraminiferal assemblages was performed on 22 samples collected at sites 1 and 2 (Figs 2a, 2c and 3) where hemipelagic marls of the Case Gallo Formation crop out. The absence of marly strata at sites 3 and 4 (Figs 2a and 3)

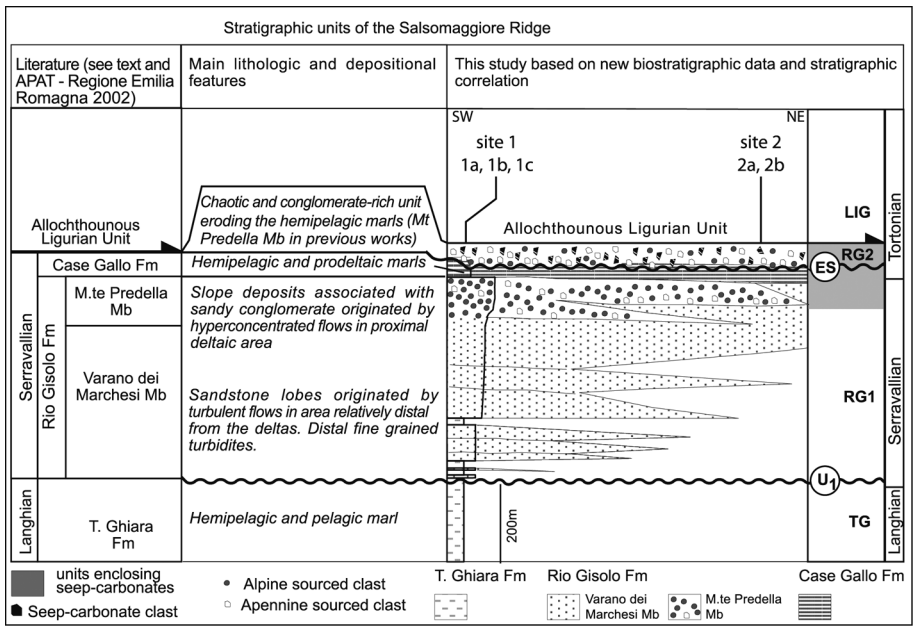

Fig. 3 - Synthetic stratigraphic column of foredeep deposits exposed in the Salsomaggiore Structure close to the studied sites 1-2. The local stratigraphic units recognized in this study (on the right) are compared with the lithostratigraphic units (on the left). The studied seep-carbonates occur within the upper part of the unit RG1 and in unit RG2 (shaded grey area). (Modified after Zanzucchi et al. 2000; APAT-Regione Emilia Romagna 2000; unpublished data of Piola 2003).

prevented any biostratigraphic analysis. Samples were dehydrated in an oven, treated with diluted hydrogen peroxide and washed through a 63 μm sieve. Although a terrigenous component is common, microfossils are abundant and planktonic foraminifera are only slightly re-crystallized. A semi-quantitative biostratigraphic analysis was carried out on the >125 μm fraction of the washed residue, and was based on surveying a standard number (9) of fields in a rectangular picking tray. Eleven taxa that are known to have biostratigraphic significance were considered and the following abundance categories were distinguished: Trace (< 3 specimens in 9 fields), Rare (3 to 10 specimens), Common (10 to 30 specimens), and Abundant (> 30 specimens). Biostratigraphic interpretation is based on: 1) the occurrence of marker species, whose first and/or last occurrences identify zonal and/or subzonal boundaries in the Mediterranean zonation of Sprovieri et al. (2002); and 2) the abundance patterns of marker species compared with that recorded in other Mediterranean astronomically tuned successions (e.g., Hilgen et al. 2000, 2003; Foresi et al. 2002; Lirer et al. 2002) which provide very accurate astronomical ages for all of the bioevents. Lourens et al. (2004) and Hüsing et al. (2007) refined age estimates of the bioevents using the astronomical solution La2004 of Laskar et al. (2004). In this study, we refer to the biostratigraphic record of Monte Gibliscemi section (Sicily, southern Italy) which also provides a $\delta^{18}O$ record of the late Serravallian-early Tortonian time interval in the Mediterranean (Turco et al. 2001).

25 geochemical analyses ($\delta^{13}C$ and $\delta^{18}O$ isotopes) performed on 18 samples of different sites around the Salsomaggiore Ridge are reported in Table 1. The $CaCO_3$ samples were finely ground in an agate mortar and aliquots of about 8-10 mg were roasted in vacuo at 350±10°C for 45 min to pyrolize the organic matter that may have been present in the samples. After roasting, the samples reacted overnight at 25°C with 100% H_3PO_4 and the released CO_2, after cryogenic purification, was measured by means of a Finnigan Delta S mass spectrometer against a laboratory sub-standard CO_2 gas obtained from a very pure Carrara marble. The isotopic values are reported in the usual delta terminology where δ is defined by the following relationship:

$$\delta=[(Rsa:-Rst)/Rst:] \times 10^3$$

where Rsa is the isotopic ratio ($^{13}C/^{12}C$ or $^{18}O/^{16}O$) in the sample and Rst is the same isotopic ratio in the standard gas. All the samples were run in duplicate and the reported values are the mean of two concordant results. All the analyses were calibrated versus international standard references periodically tested (NBS-19, NBS-20 and PDB-1).

Results

Facies of seep-carbonates of the Salsomaggiore Ridge

At the four sites of SR, the seep-carbonates generally consist of irregular, calcareous bodies, pods and lenses associated with carbonate breccias, and often contain abundant seep-related bivalves. Conglomerates and coarse sandstones are commonly cemented by authigenic micrite and are a dominant feature at some stratigraphic levels. In the present work, the data of Conti et al. (2007) are synthetized and three main lithofacies are distinguished on the basis of the prevailing lithology and the isotopic signature of carbonates (Tab. 1); new details on sedimentary features are reported in Fig. 4.

Lithofacies 1 consists of marly to arenaceous breccias (Fig. 4A-a) and conglomerate beds that are cemented and encrusted by seep-carbonates (Fig. 4A-a, b). Cement is pervasive throughout many beds (Fig. 4A-c) and locally fills veins (Fig. 4A-d). Lithofacies 1 occurs within the Monte Predella and Varano dei Marchesi Members. Compared to the other lithofacies, the carbonate isotopic signature of lithofacies 1 shows the highest $\delta^{13}C$ and always positive $\delta^{18}O$ values (Tab. 1). Lithofacies 1 has been generally associated with slow seepage mode (Conti et al. 2007).

Lithofacies 2 is mainly made up of limestones (Fig. 4A-e), marly and arenaceous limestones with densely packed bivalves (Fig. 4A-f) and carbonate breccias that locally alternate with sandstone and sporadic conglomerate lenses. This lithofacies is included within the hemipelagic and prodeltaic marls (Case Gallo Formation) and rarely is associated with sandstones or conglomerates of the Varano dei Marchesi Member. Lithofacies 2 has the largest thickness (about 2-3 m), areal

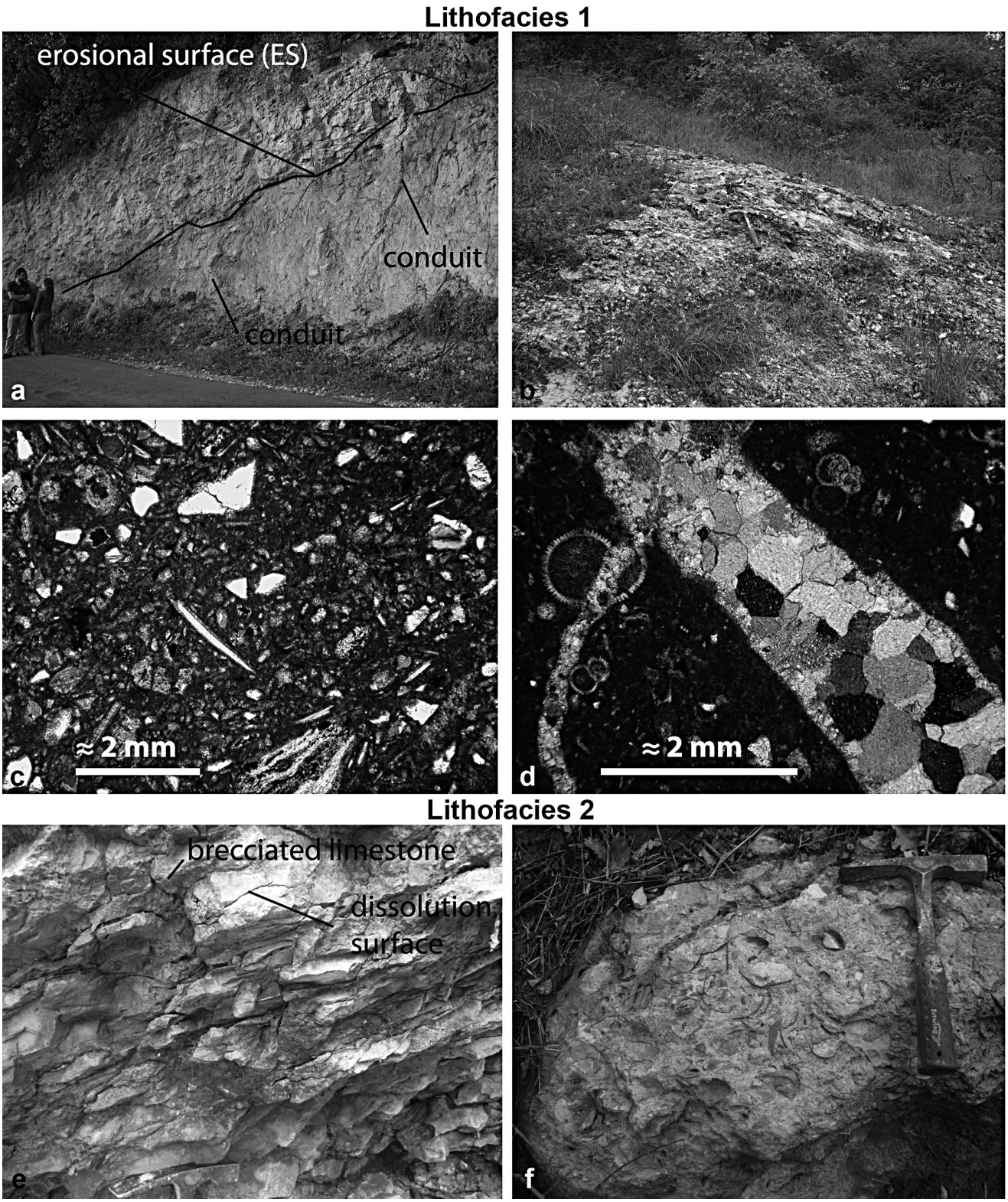

Fig. 4A - Lithofacies of seep-carbonates of the SR. **Lithofacies 1**- a) Marly-arenaceous breccias and conglomerate beds cemented by seep-carbonates; locally, feed cement-filled conduits are cemented and pass through different stratigraphic units. Here, the erosional surface (ES) between RG1 and RG2 units (see p. 327 and Fig. 7) can be observed. b) Conglomerate bed encrusted by seep-carbonate. Hammer for scale (≈ 35 cm). c) Pervasive cementation of sandstone. d) Veins filled with multiple precipitation generations of sparry calcite; this cement can also occur in other lithofacies. **Lithofacies 2** - e) Limestone and marly limestones with lenticular bedding, local dissolution features and, not clearly visible, fine-grained brecciated carbonates (lithofacies 3) along veins cross-cutting the bedding. This carbonates laterally interfingers with marls of the Case Gallo Formation. (RG1). f) Marly and arenaceous limestones with densely packed bivalves in a chemosynthetic epifaunal association (*Lucina* sp). A typical "*Lucina* limestone" with both open and closed (life position) valves. This facies indicates the position of the paleo-seafloor.

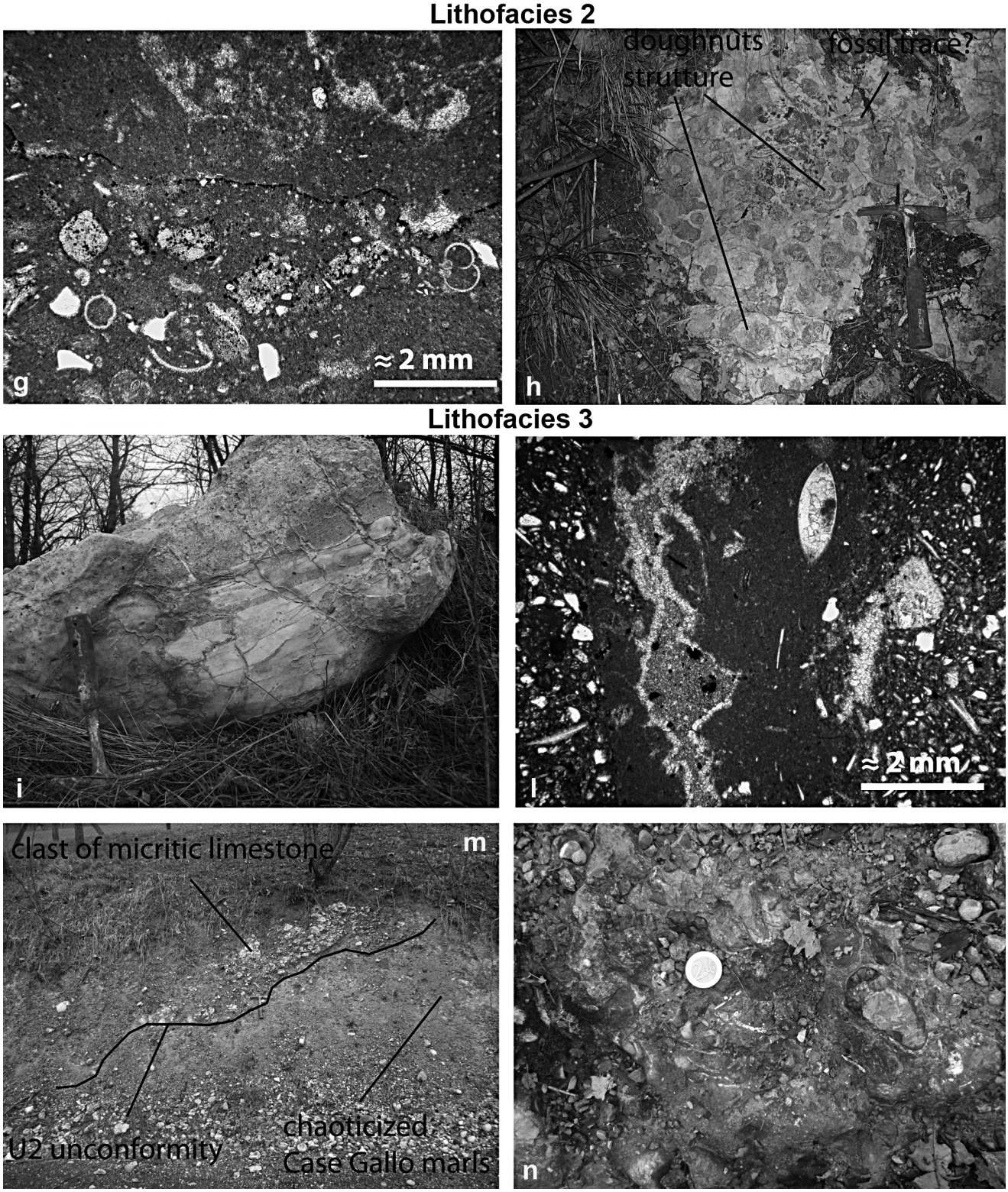

Fig. 4B - Lithofacies of seep-carbonates of the SR. **Lithofacies 2 –** g) Fossiliferous micrites with small bivalves and foraminifera casts. h) Calcarenites and marly arenites with expulsion-related conduits; doughnuts and small tubes are visible. The former are conduits through which sandstone (dark grey spots) moves upward and form concentric rings cemented by white micrite. The small tubes are probably related to traces of fossils. **Lithofacies 3** - i) Monogenic and polygenic breccias eroding a bedded limestone layers (lithofacies 2) with lenses of coarse-grained calcarenite; both lithologies are cross-cut by a dense network of veins and autoclastic fractures filled by sedimentary carbonates sediments and diagenetic calcite. l) Calcarenite and fossiliferous limestone with centimetric wide fracture filled with calcite and fossiliferous limestone; in the middle of this vein, there is a younger vein with irregular shape filled with sparry calcite on the walls and micritic calcite in the center. m) Base of the metric to decametric "topmost chaotic unit", comprising reworked seep-carbonate blocks with soft-sediment deformation, blocks of hemipelagic marls, pebbly sandstones and polygenic conglomerates in the Case Cantoniera section (2a in Fig. 5). n) Conglomerate of Monte Predella Mb. (RG2 unit) cemented by seep-carbonates; locally, lucinid-like clams are associated with this cemented conglomerate.

	LITHOFACIES	STRUCTURES	IMAGE	SAMPLE*	δ 13C (‰)	δ 18° (‰)
1	a) marly-arenaceous breccia, conglomerate	pervasive cementation and vein filling	Figs.: 4a, c, d	FL15	-8.74	+0.95
	b) marly-arenaceous breccia, conglomerate	encrustation	Fig.: 4b	CM1-08-1	-26,69	+1.47
2	a) fossiliferous micritic limestone and calcarenite	oligotypical densely packed faunal assemblage in life position, fluid-expulsion-related conduits	Figs.: 4f, 4g	CM3-08-1, Va1,Va3, CM5- 08A, CM5-08B	from -23,84 to -35.43	from -2.42 to + 0,19
	b) marly limestone and calcarenite	lamination, dissolution features	Fig.: 4e	FL17b, CM2-08	from -18.75 to -28.74	from +1.39 to +1.86
	c) micritic limestone	extensive vuggy fabrics, complex networks of cavities	Fig.: 4e	FL1, FL4, CM3, CM6-08	from -30.12 to – 4.65	from +0.01 to +0.93
	d) mottled limestone	irregular association of centimetric tubes, bioturbations and doughnut structures associated to centimetric or smaller veins filled by sparry calcite	Figs.: 4d, 4h	CM3-08-2, CM3-08-3, PG491b	from -21.76 to – 23.57≈	from -1.01 to – 0.73
	e) marly limestone	dense networks of carbonate-filled veins and autoclastic fractures (millimeter to centimeter wide)	Figs.: 4i, 4l	FL3, PG 491a	from -31.09 to -34.48	from +0.23 to +0.25
	f) monogenic and poligenic breccia	erosional, vein forming	Figs.: 4e, 4i	490°, 490b, CM2, CM4-08-1, CM4-08-2, CM4-08-3	from -28.06 to -34.39	from -1.05 to +0.89
3	poligenic conglomerate with seep-carbonate clasts	erosional, soft-sediment deformation, chaotic	Figs.: 4m, 4n	PG487	-41.43	+2.85

Tab. 1 - Summary of the sedimentary features and geochemical signature of the main lithofacies of the SR seep-carbonates. The geochemical results of 15 samples derive from Conti et al (2007); the three additional samples (CM1, CM4, CM6 from Case Mezzadri site) provide similar geochemical signature as the 15 samples analysed in the previous work. From lithofacies 1 to 3, the seepage mode passes from a prevailing slow- to a prevailing fast-seepage. Nonetheless, vein formation and carbonate cements are common to the three lithofacies and they may represent either fast or slow-seepage mode. See also text and Fig. 4. * See Fig. 9 and Table 1 in Conti et al. (2007).

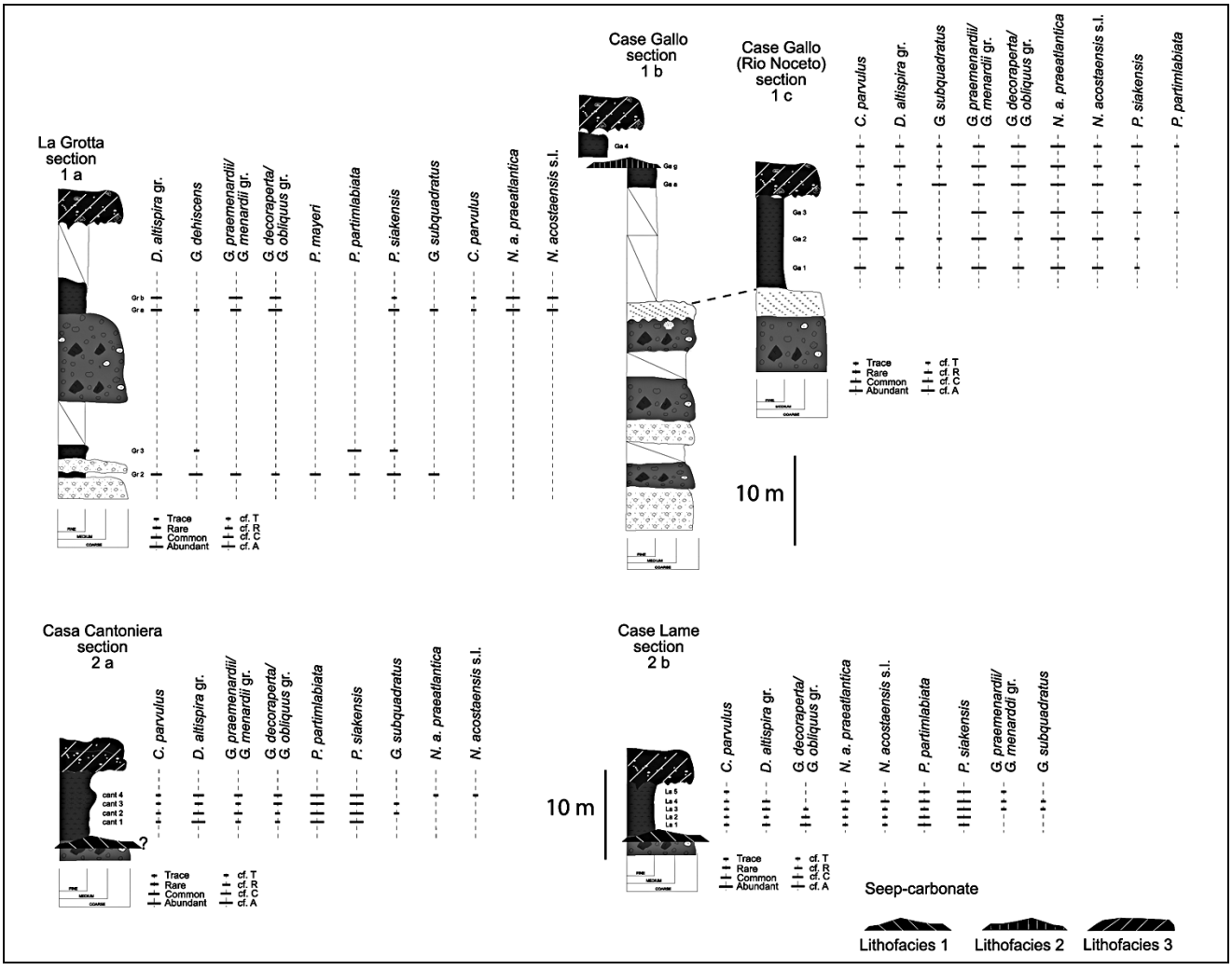

Fig. 5 - Distribution range of planktonic foraminiferal species in the stratigraphic sections located at sites 1 and 2. Sample positions (e.g., Gr a, etc.) are reported on the right of the stratigraphic columns. Four sections (1a, 1b, 2a, 2b) are partially modified after Piola (2003) and Conti et al. (2007), while section 1c is documented for the first time.

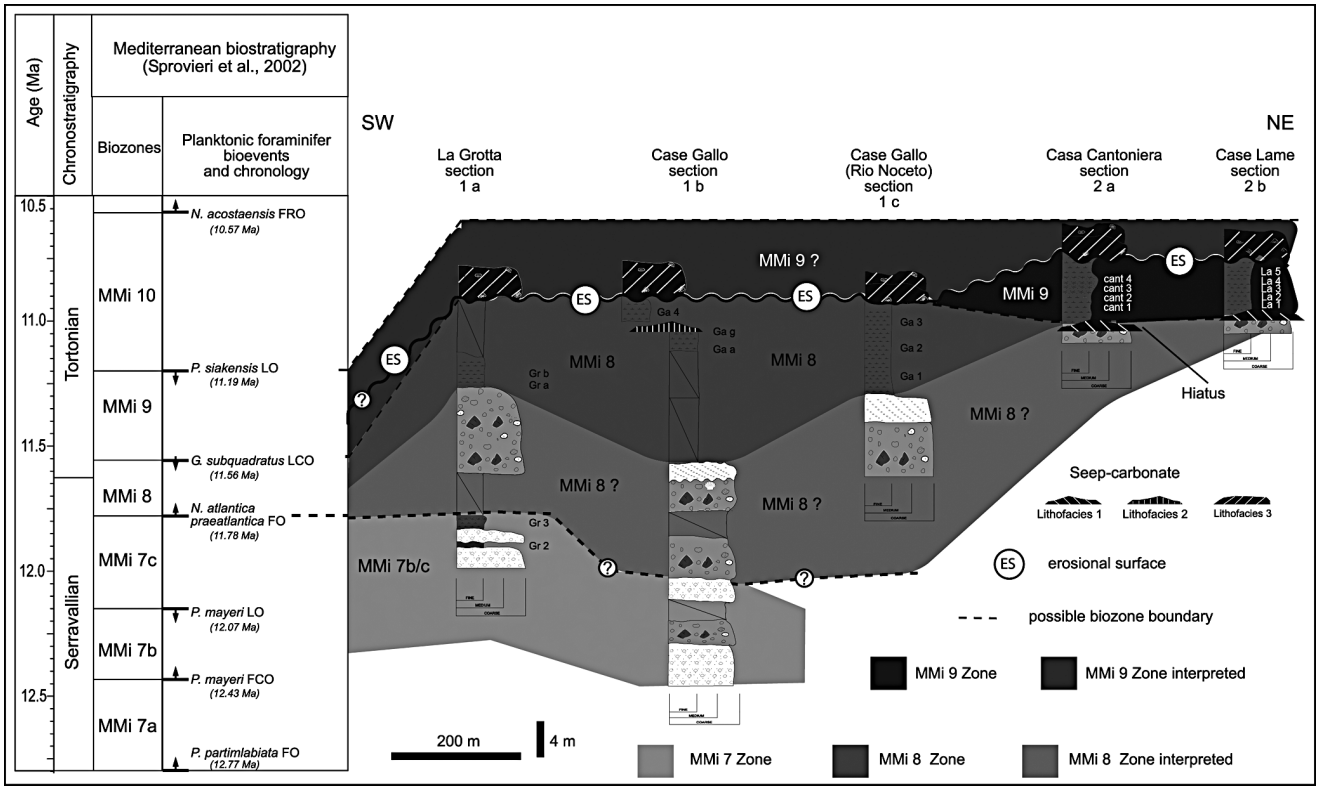

Fig. 6 - Biostratigraphic interpretation and stratigraphic correlation of the studied sections containing hemipelagic marls. The planktonic foraminifer zonation of Sprovieri et al. (2002) has been adopted in this study. Absolute ages of the main bioevents are also reported (after Lourens et al. 2004). The age of the bioevent which defines the MMi7b/MMi7c subzonal boundary has been recalibrated after Hüsing et al. (2007).

extent (maximum 200 m^2), and lithology variability. On the basis of lithology, this lithofacies can be subdivided into 6 sublithofacies which also reflect variable isotopic values (Tab. 1). Lithofacies 2 shows the $\delta^{13}C$ minimum values (between -23.84‰ and -35.43‰ $\delta^{13}C$ PDB-1) and $\delta^{18}O$ mainly around 0‰; slightly negative $\delta^{18}O$ values (between -0.73‰ and -2.42‰ $\delta^{18}O$ PDB-1) are associated with sublithofacies 2a, 2d and 2f. Lithofacies 2 has been mainly related to slow-seepage fluid emission (Conti et al. 2007).

Lithofacies 3 is a chaotic facies, made up of blocks of reworked seep-carbonates (Fig. 4B-i-n), blocks of hemipelagic marls, pebbly sandstones and polygenic conglomerates cemented by seep-carbonates (Fig. 4B-n). Clasts of seep-carbonates often show soft-sediment deformations (Fig. 4B-m). Lithofacies 3 (Fig. 4B-m, n) occurs in the Monte Predella Member and mainly in the "topmost chaotic unit" (Figs 3 and 4B-m). One isotopic datum from calcite in lithofacies 3 gave the lowest value of $\delta^{13}C$ (-41,43‰ PDB-1) and highest $\delta^{18}O$ (2,85‰ PDB-1); this facies has been related to fast seepage mode of fluid expulsion (Conti et al. 2007).

Biostratigraphic age constraints of the seep-associated deposits

The results of the planktonic foraminiferal analysis and the biostratigraphic interpretation of the studied sections at sites 1 and 2 are presented in Figs 5 and 6, respectively.

In the La Grotta section (1a), the assemblage from the lowermost marls (sample Gr 2) is characterized by the occurrence of *Paragloborotalia partimlabiata*, *P. siakensis* and *P. mayeri* (Fig. 5). The co-occurrence of these species indicates that the lowermost part of the La Grotta section belongs to Subzone MMi7b (Fig. 6). This subzone is Serravallian in age ranging from 12.43 Ma to 12.07 Ma (Hüsing et al. 2007). In the overlying marls the co-occurrence of *P. partimlabiata* and *P. siakensis*, and the absence of *P. mayeri* (sample Gr 3) may indicate either Subzone MMi7b, if the absence of *P. mayeri* is due to its discontinuous occurrence within its distribution range (see Foresi et al. 2002; Lirer et al. 2002; Hilgen et al. 2003), or Subzone MMi7c if the species is already extinct (Fig. 6). The uppermost hemipelagic marls in the La Grotta section yield an assemblage mainly characterized by the occurrence of randomly coiled *Neogloboquadrina atlantica praeatlantica* (= *N. atlantica* small size in Hilgen et al. 2000, 2003; Turco et al. 2001) and *N. acostaensis* s.l. This assemblage is referable to Zone MMi8, which coincides with the first influx of neogloboquadrinids characterized by a random coiling direction and ranges from the First Occurrence (FO) of *N. atlantica praeatlantica* (dated at 11.78 Ma) up to the Last Common Occurrence (LCO) of *Globi-*

gerinoides subquadratus (dated at 11.56 Ma; Lourens et al. 2004) (Fig. 6). The latter bioevent approximates the Serravallian/Tortonian boundary (Hilgen et al. 2005), recalibrated at 11.625 Ma (Hüsing et al. 2007) (Fig. 6). After the LCO of *G. subquadratus*, neogloboquadrinids are nearly absent in the Mediterranean, but re-appear as predominantly dextrally-coiled forms at 11.15 Ma (Hilgen et al. 2000; Foresi et al. 2002; Lourens et al. 2004). In summary, deposition of the hemipelagic marls in the La Grotta section started during the Serravallian and possibly ended in the early Tortonian, and the maximum age of these strata ranges between 12.43 Ma (*P. mayeri* First Common Occurrence – FCO) and 11.56 Ma (*G. subquadratus* LCO) (Fig. 6).

In the Case Gallo sections (1b and 1c), hemipelagic marls overlying the conglomeratic strata yield assemblages characterized by abundant randomly coiled neogloboquadrinids with *N. atlantica praeatlantica* prevailing on *N. acostaensis* s.l., associated with *G. subquadratus* and *Catapsydrax parvulus*; *P. siakensis* and *P. partimlabiata* are generally rare and not typical (Fig. 5). This assemblage is referable to Zone MMi8. Therefore, the hemipelagic marls in the Case Gallo section are also Serravallian-early Tortonian in age, but their maximum age is younger, ranging from 11.78 Ma to 11.56 Ma (Fig. 6).

In the Casa Cantoniera and Case Lame sections (2a and 2b, respectively), the assemblages are very similar in taxonomic composition (Fig. 5). They consist of abundant *P. siakensis* and *P. partimlabiata* (=*P.* cf. *partimlabiata* in Foresi et al. 2002), rare neogloboquadrinids and very rare *G. subquadratus*, and they are referable to Zone MMi9 (Fig. 6). This biozone is defined as the stratigraphic interval between the LCO of *G. sub-*

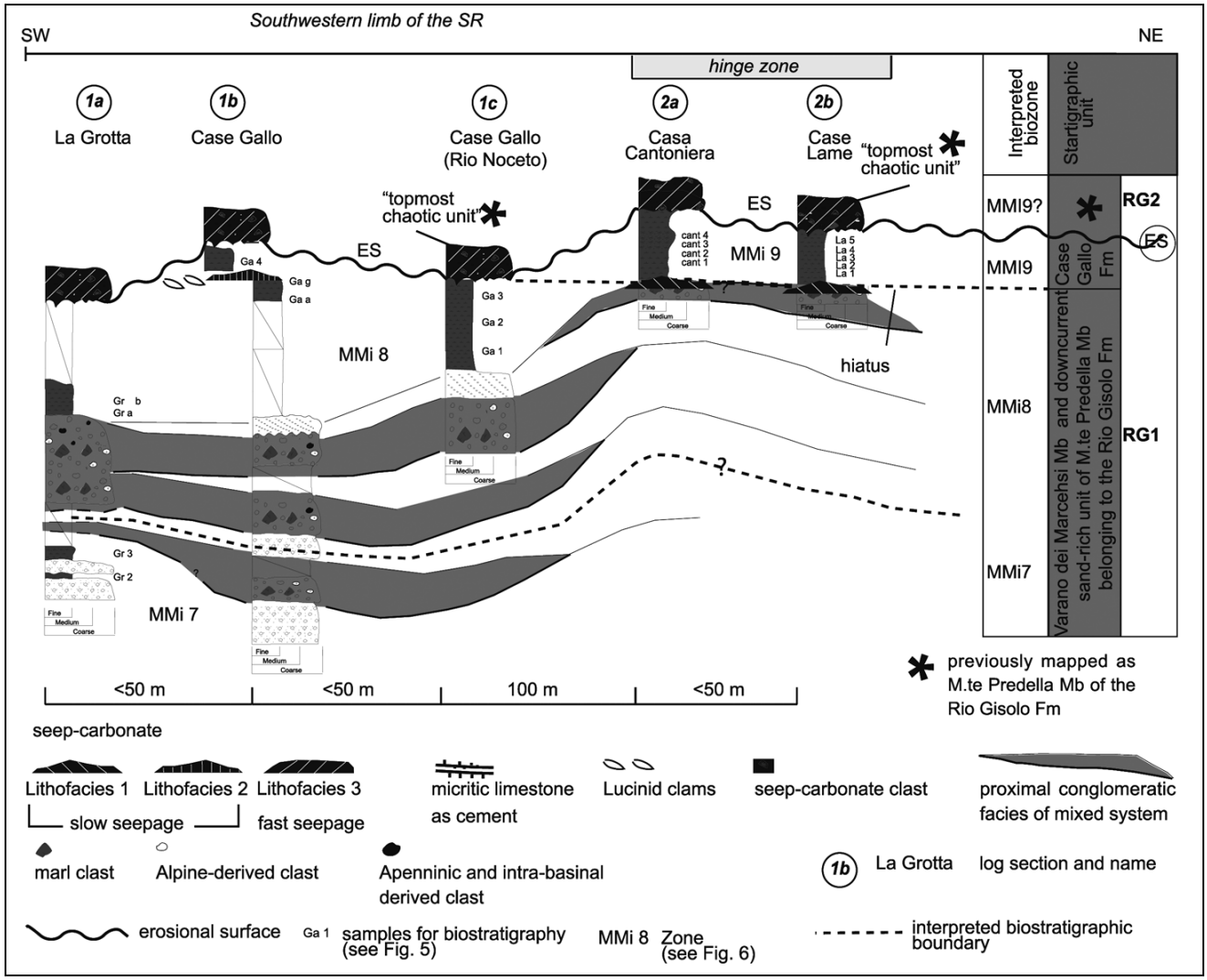

Fig. 7 - Composite stratigraphic panel showing the updated stratigraphic framework for the SR based on stratigraphic correlation and new biostratigraphic data (see Fig. 6) from sites 1 and 2. The position of the seep-carbonates is reported on the stratigraphic sections. Note: 1) the proximal facies of the mixed systems deposits prograde north-eastward; 2) the hemipelagic marls are becoming younger and partially missing (hiatus) toward the SR's hinge zone; 3) the erosional surface (ES) is the base of the RG2 unit or "topmost chaotic" unit of Conti et al. (2007).

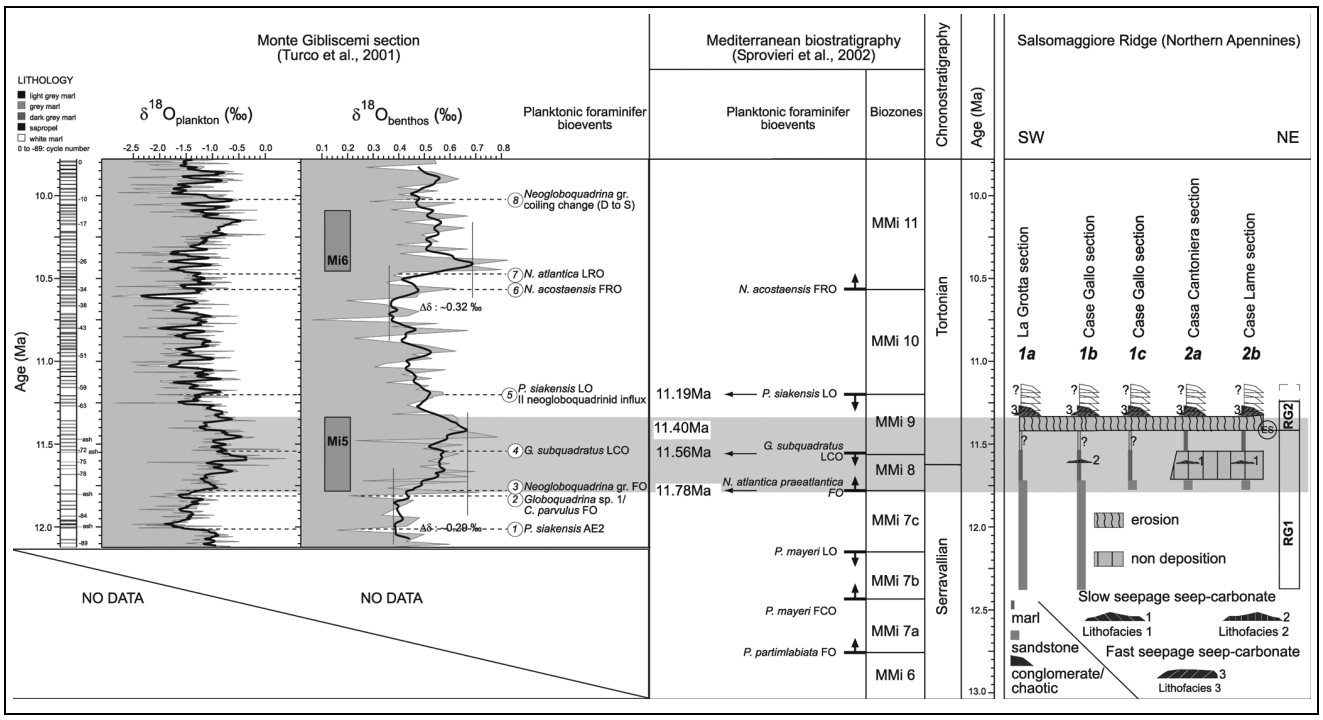

Fig. 8 - Oxygen isotope records, based on planktonic ($\delta^{18}O_{pl}$ (‰)) and benthic ($\delta^{18}O_{be}$ (‰)) foraminifera, and planktonic foraminiferal events which constrain Mi5 and Mi6 global cooling events at Monte Gibliscemi (Italy) (Turco et al. 2001) used as reference section in this study (figure modified after Turco et al. 2001). Biostratigraphic zonation of Sprovieri et al. (2002) and absolutes ages of bioevents. Chronostratigraphy of the studied stratigraphic sections (for complete sections see Figs. 5, 6, 7). Note that seep-carbonates are coeval with the Mi5 cooling event.

quadratus and the Last Occurrence (LO) of *P. siakensis* (dated at 11.19 Ma). This biostratigraphic assignment indicates that the hemipelagic marls at Casa Cantoniera and Case Lame are early Tortonian in age and younger than those of the Case Gallo section.

Updated stratigraphic framework of the seep-carbonates of the growing Salsomaggiore Ridge

Sedimentary facies and biostratigraphic interpretation of the sections, logged through the upper part of Rio Gisolo and Case Gallo Formations, made it possible to refine the stratigraphic framework of the rocks encasing the seep-carbonates (Figs 3, 5, 6 and 7). This stratigraphic framework, however, is based only on sites 1 and 2, because no datable marls are present at sites 3 and 4 and the mixed-system deposits of sites 3 and 4 cannot be correlated with certainty either with the mixed-system deposits or with the hemipelagic marls of sites 1 and 2.

Biostratigraphic interpretation of planktonic foraminiferal assemblages indicates that the hemipelagic marls of the Rio Gisolo and Case Gallo Formations are referable to the time interval between Zone MMi7b/c and Zone MMi9 (Serravallian to early Tortonian), with a maximum time span between 12.43 Ma and 11.19 Ma (Figs 6, 7, 8). The position of MMi7/MMi8 and MMi8/MMi9 zonal boundaries is inferred (Fig. 6) because of discontinuous or lacking outcrops of the hemipelagic marls and intercalation of thick conglomerates. Biostratigraphic correlation of the studied sections, however, suggests that the hemipelagic marls of the Case Gallo Formation become younger in a SW-NE direction toward the SR hinge zone where a stratigraphic hiatus also occurs (Figs 6, 7, 8).

Moreover, these data (Figs 3, 6, 7, 8) allowed the recognition of an erosional surface (ES), which cuts the hemipelagic marls of the Case Gallo Formation (sites 1 and 2) (Figs 2c, 3, 6, 7). At site 2 (Case Cantoniera and Case Lame sections), the ES marks the boundary between the "topmost chaotic unit" of Conti et al. (2007) (upper part of Monte Predella Member) and the underlying hemipelagic marls (Case Gallo Formation) (Fig. 4m). Although outcrop conditions did not allow to trace it throughout the study area (Fig. 2a), this erosional surface may represent a major stratigraphic boundary in the SR succession before the emplacement of the allochthonous units (see Geological setting). The unconformity U1 and the ES, therefore, allowed the subdivision of the middle-upper Miocene succession of the SR into three local stratigraphic units. These units are: 1) TG unit, not investigated here, which corresponds to the Torrente Ghiara Formation; 2) RG1 unit (MMi7b/c-MMi9 Zones) which includes the lower part of the Rio Gisolo Formation and the Case Gallo For-

mation; 3) RG2 unit (MMi9? Zone) which corresponds to the "topmost chaotic unit" of Conti et al. (2007) (Figs 2, 3 and 7).

The growth of the Salsomaggiore Ridge

On the basis of the updated stratigraphic framework a syn-depositional uplift of the SR is suggested to occur in two stages.

The first stage is represented by unit RG1 (Figs 3, 7) ranging from late Serravallian up to early Tortonian in age (Subzones MMi7b/c-Zone MMi9). In the lower part of RG1 (Subzones MMi7b/c and possibly Zone MMi8), sandy and conglomeratic deposits show an overall coarsening-upward. This trend testifies the north-eastward progradation, toward the anticline hinge zone, of the proximal facies belonging to the mixed systems (*sensu* Mutti et al. 2003) (Figs 6, 7). Such a shift appears to be strictly related to the uplift of the crestal area of the SR (Artoni & Tinterri 2009) as it typically occurs in a structurally-controlled foredeep (Muzzi Magalhaes & Tinterri 2010; Tinterri & Muzzi Magalhaes 2011).

Afterward, hemipelagic and prodeltaic marls of unit RG1 (Case Gallo Formation), deposited in Zone MMi8 and part of Zone MMi9 (upper Serravallian – lower Tortonian), indicate a sharp decrease in coarse-grained clastic supply (Figs 6, 7). In proximity of the hinge zone of SR a stratigraphic non-depositional hiatus was forming: marls of Zone MMi9 directly overlie coarse-grained mixed-system deposits and marls referable to Zone MMi8 are missing (sections 2a, 2b in Fig. 7). Thus, the hiatus is suggested to have a maximum duration of 230 kyrs (i.e., duration of Zone MMi8) (Casa Cantoniera, Section 2a, Figs 6, 7, 8).

The second stage is represented by unit RG2, above the ES surface, and it corresponds to the "topmost chaotic unit", which clearly crops out at sites 1 and 2 (Figs 3, 7). The age determination of unit RG2 is problematic because no younger deposits are found above it, except for allochthonous units (Fig. 7). It is inferred that unit RG2 was deposited during the upper part of Zone MMi9, or slightly afterward, because it postdates the hemipelagic marls referable to Zone MMi9 at site 2 and it includes reworked seep-carbonates not completely lithified (soft sediment deformation structures in micritic seep-carbonate clasts derived from the underlying RG1 unit; Tab. 1).

In this updated stratigraphic framework, the three lithofacies of seep-carbonates show the following distribution. In unit RG1, lithofacies 1 and 2 occurred during Zone MMi8 (late Serravallian-early Tortonian), (Figs 6 and 7): lithofacies 1 either cemented or encrusted the marly- to coarse-grained deposits in correspondence of the non-deposition hiatus surface (sections 2a, 2b in Fig. 7); lithofacies 2 interfingered with hemipelagic marls (section 1b in Fig. 7). In unit RG2 (Zone MMi9 or slightly afterward, early Tortonian), above the ES erosional surface, only lithofacies 3 can be recognized (Fig. 7).

Discussion

Tectonic control on seepage: the case of the Salsomaggiore Ridge

Tectonics is an important trigger for fluids accumulation and mobility in compressional structures. Progressive folding or thrusting are generally associated with formation of multiple generations of fractures, close to the buried thrust tip or at the crest of an anticline. In fact, thrust faults and anticline crests are known as preferential locations of hydrate accumulation and/or dissociation (Le Pichon et al. 1992; Tréhu et al. 1999, 2004, 2006; Sassen et al. 2001; Schwartz et al. 2003; Aiello 2005; Weinberger & Brown 2006). In appropriate temperature and pressure conditions for gas hydrates formations, migration of fluids along fractures may result in the formation of hydrate seals and trapping of methane in the underlying strata (Reed et al. 1990; Trehu et al. 1999; Aloisi et al. 2000; Wiedicke et al. 2002). The rupture of the hydrate seal by tectonic activity allows methane to flow along fractures and contribute to fluid expulsion that might be released in a short time or abruptly even during an earthquake swarm (Fischer et al. 2013). Rapid release of fluids can cause fluid overpressure, which, in association with the low shear strength of surficial sediments, induces instability processes, such as sliding, slumping and chaotic deposits (Maslim et al. 1998, 2004, 2005; Percher et al. 2001; Mienert et al. 2004).

During the late Serravallian-early Tortonian time interval, the SR anticline's hinge zone experienced both local and regional tectonic pulses, which likely contributed to fluid mobilization and hydrate dissociation (Figs 6, 7). Local tectonic activity resulted in uplift, subtle growth and presence of a submarine relief, also suggested by lateral facies associations of mixed systems (Artoni & Tinterri 2009). Regional-tectonic activity involved Ligurian and epi-Ligurian allochthonous units, which advanced in different steps (Ricci Lucchi 1986; Pini 1999). These allochthonous units arrived in proximity of the SR during deposition of the seep-carbonates, as evidenced by the increase in Apennine-sourced clasts cemented by seep-carbonates inside the unit RG2 (Figs 2, 3, 7) (Conti et al. 2007). During this advancing pulse, the allochthonous units should have had a wedge shape similar to the present-day geometry (thickness passing from 4 to 0 km over a distance of 20 km in a SSW-NNE direction) (Artoni et al. 2010; Carlini et al. 2013). This wedge created a differential load on the underlying fore-

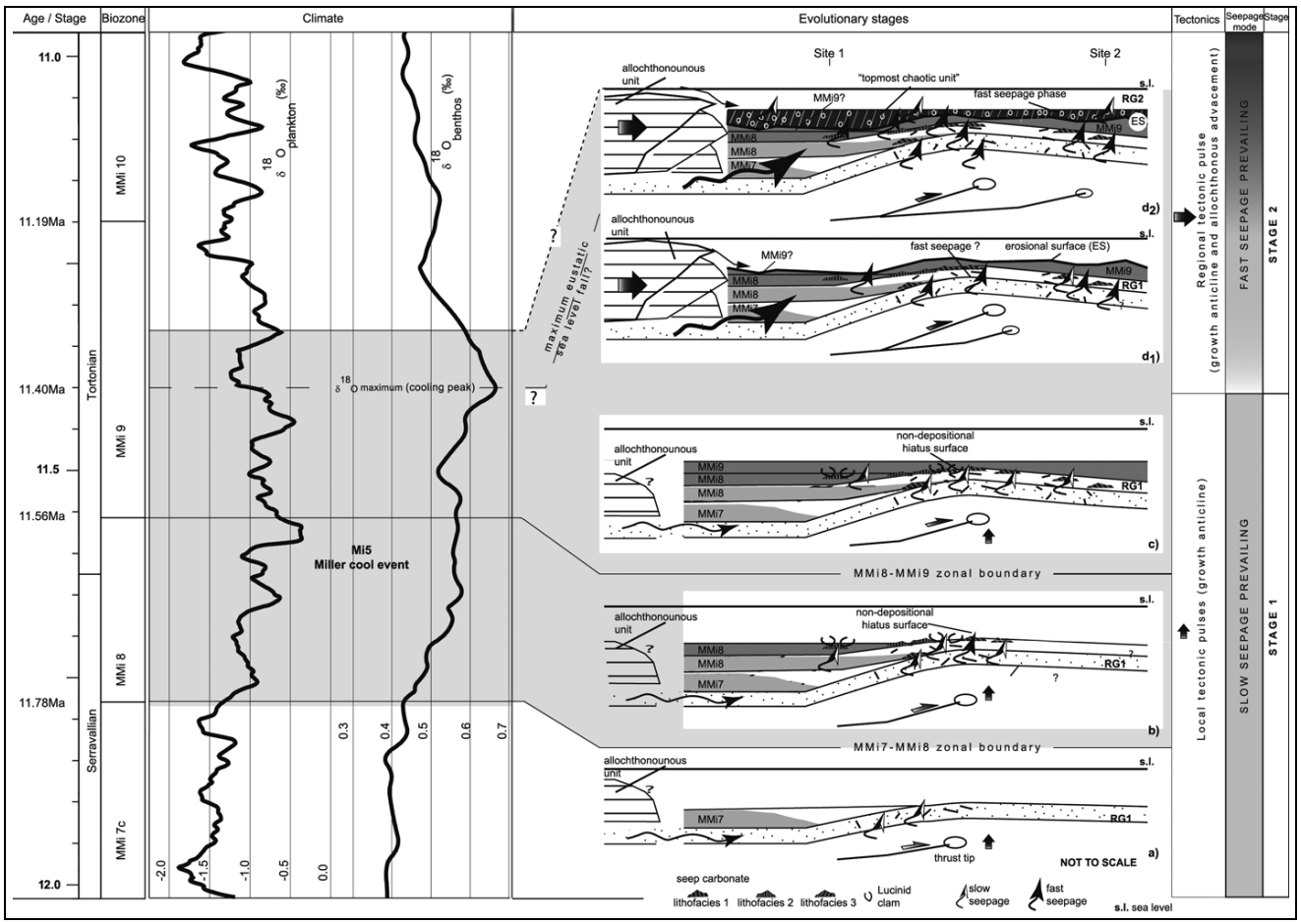

Fig. 9 - The two-stage evolution model of fluid-seepage and associated carbonate deposits in the Salsomaggiore Ridge during the late Serravallian (a-b) and early Tortonian (c, d_1, d_2), related to both tectonics (on the right) and climate change (oxygen isotope record on the left). Oxygen isotope curves of planktonic ($\delta^{18}O_{pl}$ (‰)) and benthic ($\delta^{18}O_{be}$ (‰)) foraminifera are from Turco et al. (2001) (see also Fig. 8). Seepage mode is also shown on the right and is based on the main recognized lithofacies (see Fig. 4, Tab. 1 and Conti et al. 2007). Seepage appears to be controlled by both tectonics and climate changes.

deep units. The resulting lateral lithostatic gradients should have forced fluids to migrate from the south (where the allochthonous wedge was thicker and the lithostatic load higher) to the north, i.e. towards the developing SR (where the allochthonous wedge was thinner and the lithostatic load smaller). In the crestal area of SR, both the porous coarse-grained deposits (primary porosity) and the fracture network (secondary porosity) represented the preferential locations for fluids to be trapped, expelled or become caught up in surficial slope instability. Thus, the SR crestal zone became site of seepage and carbonate precipitation.

Climatic control on seepage: the case of the Salsomaggiore Ridge

The late Serravallian to early Tortonian time interval (Zone MMi8-Zone MMi9) is characterized by a global cooling event, namely Mi5 (Miller et al. 1991a, 1991b) (Fig. 8). This climatic event is marked by an increase of the $\delta^{18}O$ oxygen isotope both in the open ocean (e.g. Miller et al. 1991a; Wright & Miller 1992; Shackleton & Hall 1997) and in the Mediterranean (Turco et al. 2001). In the Monte Gibliscemi section (Italy), the cooling trend started at 11.8 Ma, coinciding with the base of Zone MMi8 and culminated at 11.4 Ma (maximum cooling) within Zone MMi9 (Fig. 8).

The Mi5 event is associated with a glacio-eustatic sea level lowering of 30-45 m (Miller et al. 1991b). These authors suggested a causal relationship between the isotopic events and the timing of erosional events (unconformities), due to ice volume growth and global sea level lowering; as a matter of fact, erosional unconformities preferentially develop during the highest rates of eustatic sea level falls (Haq et al. 1988; Posamentier & Vail 1988) related to climate changes (Warrick et al. 2009). Maxima in $\delta^{18}O$ would then correspond to the most extreme lowstands similarly to Pleistocene oxygen marine isotopic stages (MIS) corresponding to eustatic sea-level changes (Shackleton & Matthews 1977; Shackleton 1987).

Eustatic sea level changes, and consequentially pressure changes, might induce dissociation of hydrates

as they move away from their stability zones (Kvenvolden 1993) and trigger catastrophic sediment failures which generate mass-transport deposits (Maslim et al. 1998, 2004, 2005; Katz et al. 1999; Percher et al. 2001; Bohrmann et al. 2002; Mienert et al. 2004).

At SR, in unit RG1, during Subzones MMi7b/c, there is no evidence of seep-carbonate deposition, while during Zone MMi8 lithofacies 1 and 2 started to form during the onset of the Mi5 event. In unit RG2, possibly during Zone MMi9, the seep-carbonates occur above the erosional surface ES. Such a surface might be reasonably associated with the eustatic sea level drop and not only with the regional tectonic pulse. It is hypothesized that seep-carbonates, represented by lithofacies 3 might have formed around the culmination of Mi5 cool event (benthic foraminifer $\delta^{18}O$ maximum at 11.4 Ma).

The evolution of seep-carbonate deposition at the Salsomaggiore Ridge

The updated stratigraphic framework, the stratigraphic distribution of the seep-carbonates and the relationship with tectonic activity (local and regional) and Mi5 glacial event constrain a two-stage model for seep-carbonate deposition at SR (Fig. 9).

In the first stage, during Zone MMi7 (Fig. 9a), subtle growth of the SR and the creation of local submarine relief controlled deposition of mixed-system sediments of RG1 unit. Continuous and progressive deformation at the SR crestal area and its limbs produced fracture networks that cross-cut porous, coarse- and fine-grained deposits of unit RG1. The combination of tectonic activity and lithology represented an ideal framework for fluid migration, trapping and expulsion. Still in the first stage, the onset of Mi5 cool event (base of Zone MMi8) occurred (Fig. 9b). During Zone MMi8 (Fig. 9b), seep-carbonates started to be deposited either encrusting or cementing coarse-grained deposits or interfingering with hemipelagic marls (Lithofacies 1, 2) (Fig. 9b). These lithofacies are mainly indicative of slow-seepage mode of seep-carbonate deposition (Conti et al. 2007). Local tectonic activity continued during deposition of the sediments hosting seep-carbonates and a local stratigraphic hiatus occurred in proximity of the anticline hinge zone (Figs 7, 8, 9b, c).

The first stage ended when the shelf to slope hemipelagic deposition was interrupted by a more intense regional tectonic pulse, which caused the advancement of the Ligurian and epi-Ligurian units toward the SR (Artoni et al. 2010) and the formation of the erosional surface (ES) (Figs. 6, 7, $9d_1$). These events mark and characterize the second stage when a renewed seepage allowed the deposition of chaotic facies with Apennine-sourced clasts and the increase of sediment instability on the flank of the SR (Lithofacies 3) (Fig. $9d_2$). The "topmost chaotic unit" (Lithofacies 3) or unit RG2 (Fig. $9d_2$) was probably linked to increased tectonic activity and possibly to the most extreme eustatic sea level fall associated to the coolest peak of the Mi5 event (11.40 Ma, Turco et al. 2001). At this stage, tectonics and climate could have concurred to enhance the rate and intensity of submarine erosion and fluid expulsion with fast seepage modality (Figs. $9d_1$, d_2). However, because of the limitations in dating unit RG2 (see § above 5) it cannot be excluded that only tectonics might have acted in this stage.

Conclusions

The study of the seep-carbonates at Salsomaggiore Ridge (SR) provides new insights on the role of tectonics, climate change and associated eustatic sea level fall in the deposition of seep carbonates.

An integrated sedimentological and biostratigraphic study of middle-upper Miocene deposits exposed at Salsomaggiore Ridge provides an updated stratigraphic framework for seep-carbonate lithofacies. Planktonic foraminiferal biostratigraphy assigns the seep-carbonates to the late Serravallian-early Tortonian time interval (Zones MMi8 and possibly MMi9 of Sprovieri et al. 2002).

Three lithofacies of seep-carbonates are defined. These lithofacies are associated with two main stages and intensities of seepage that developed during specific tectonic and climatic conditions.

In the first stage, slow seepage, characterized by carbonates of the Lithofacies 1 and 2, took place during Zone MMi8 in the early phase of the Mi5 cooling, when tectonic activity was mildly and locally modifying the Salsomaggiore Ridge.

In the second stage, fast seepage is associated with more chaotic deposits (Lithofacies 3) possibly during Zone MMi9. This second stage is related to a regional tectonic pulse that created the erosional surface (ES) and possibly enhanced eustatic sea level fall associated with more extreme climatic conditions (coolest peak of Mi5 event).

In the Salsomaggiore Ridge, tectonics and cooling event seem to concur to drive the deposition of seep-carbonates with different seepage mode.

Acknowledgements. The paper is part of a project funded by Università degli Studi di Parma to A. A. (Fil 2008 Growth modality of the Central-Northern Apennine since the Miocene). Our thanks to reviewers G. Della Porta and Anonymous for their comments that contributed to improve the manuscript. We would like to especially thank G. Papani who introduced us to the geology of the Salsomaggiore area. Many thanks also to A. Longinelli and P. Iacumin for providing isotopic analyses, F. Lorenzini and G. Piola for field work, A. Comelli and L. Barchi for preparing thin sections and polished slabs of rock samples, G. Gianelli for sample preparation for biostratigraphic analysis.

REFERENCES

Aiello J.W. (2005) - Fossil seep structures of the Monterey Bay region and tectonic-structural controls on fluid flow in an active transform margin. *Palaeogeogr. Palaeoclimatol. Palaeoecol.*, 227: 124-142.

Aloisi G., Pierre C., Rouchy J.M., Foucher J.P., Woodside J. & Medinaut Scientific-Party (2000) - Methane-related authigenic carbonates of eastern Mediterranean Sea mud volcanoes and their possible relation to gas hydrate destabilisation. *Earth Planet. Sci. Lett.* 184: 321-338.

APAT Regione Emilia Romagna (2000) - Foglio 198 Bardi della Carta Geologica d'Italia alla scala 1: 50.000.

Amorosi A., Colalongo M.L. & Vaiani S.C. (1993) - Le unità epiliguri mioceniche nel settore emiliano dell'Appennino settentrionale. Biostratigrafia, stratigrafia sequenziale e implicazioni litostratigrafiche. *Palaeopelagos*, 3: 209-240.

Argnani A. & Ricci Lucchi F. (2001) - Tertiary silicoclastic turbidite systems of the Northern Apennines. In: Vai G.B. & Martini I.P. (Eds) - Anatomy of an orogen: the Apennines and adjacent Mediterranean basins: 327-350. Kluwer Academic, London.

Artoni A., Bernini M., Papani G., Rizzini F., Barbacini G., Rossi M., Rogledi S. & Ghielmi M. (2010) - Mass-transport deposits in confined wedge-top basins: surficial processes shaping the messinian orogenic wedge of Northern Apennine of Italy. *Ital. J. Geosci.,* 129: 101-118. doi: 10.3301/IJG.2009.09.

Artoni A., Papani G., Rizzini F., Calderoni M., Bernini M., Argnani A., Roveri M., Rossi M., Rogledi S. & Gennari R. (2004) - The Salsomaggiore structure (Northwestern Apennine foothills, Italy): a Messinian mountain front shaped by mass-wasting products. *GeoActa*, 3: 107-128.

Artoni A., Rizzini F., Roveri M., Gennari R., Manzi V., Papani G. & Bernini M. (2007) - Tectonic and climatic controls on sedimentation in Late Miocene Cortemaggiore Wedge-Top Basin (Northwestern Apennines, Italy). In: Lacombe O., Lave' J., Roure F.M. & Verges J. (Eds) - Thrust Belts and Foreland Basins: From fold kinematics to hydrocarbon systems. Springer, Heidelberg. ISBN/ISSN: 978-3-540-69425-0, p. 431-456, doi: 10.1007/978-3-540-69426-7.

Artoni A. & Tinterri R. (2009) - Submarine orogenic front forming inside turbiditic foredeep basin: the case of the middle Miocene Salsomaggiore frontal fault-related anticline (Northern Apennines, Italy). In: AAPG Hedberg Research Conference - Butler R., Meckel T. & Peel F. (Eds) - Deepwater Fold and Thrust Belts. 4-9 October, Tirrenia (PI) Italia, Abstract Vol., AAPG Search and Discovery Article #90123©2011 http://www.searchanddiscovery.com/abstracts/pdf/2011/2009hedberg-italy/abstracts/ndx_artoni.pdf

Bangs N.L., Hornbach M.J. & Berndt C. (2011) - The mechanics of intermittent methane venting at South Hydrate Ridge inferred from 4D seismic surveying. *Earth Planet. Sci. Lett.*, 310: 105-112.

Boccaletti M., Calamita F., Deiana G., Gelati R., Massari F., Moratti G. & Ricci Lucchi F. (1990) - Migrating foredeep-thrust belt system in the Northern Apennines and Southern Alps. *Palaeogeogr. Palaeoclimatol. Palaeoecol.*, 77: 3-14.

Bohrmann G., Greinert J., Suess E. & Torres M.E. (1998) - Authigenic carbonates from the Cascadia subduction zone and their relation to gas hydrate instability. *Geology,* 26: 647-650.

Bohrmann G., Heeschen K., Jung C., Weinrebe W., Baranov B., Cailleau B., Heath R., Huhnerbach V., Hort M., Masson D. & Trumme I. (2002) - Widespread fluid expulsion along the seafloor of the Costa Rica convergent margin. *Terra Nova,* 14: 69-79.

Campbell K.A. (2006) - Hydrocarbon seep and hydrothermal vent paleoenvironments and paleontology: past developments and future research directions. *Palaeogeogr. Palaeoclimatol. Palaeoecol.*, 232: 362-407.

Campbell K.A., Farmer J.D. & Des Marais D. (2002) - Ancient hydrocarbon seeps from the Mesozoic convergent margin of California: carbonate geochemistry, fluids and palaeoenvironments. *Geofluids,* 2: 63-94.

Carlini M., Artoni A., Aldega L., Balestrieri M. L., Corrado S., Vescovi P., Bernini M. & Torelli L. (2013) - Exhumation and reshaping of far-travelled/allochthonous tectonic units in mountain belts. New insights for the relationships between shortening and coeval extension in the western Northern Apennines (Italy). *Tectonophysics*, 608: 267-287. http://dx.doi.org/10.1016/j.tecto.2013.09.029

Carminati E. & Doglioni C. (2012) - Alps vs. Apennines: the paradigm of a tectonically asymmetric Earth. *Earth Sci. Rev.*, 112: 67-96. http://dx.doi.org/10.1016/j.earscirev.2012.02.004.

Cavazza W., Roure F.M., Spackman W., Stampfli G.M. & Ziegler P.A. (Eds) (2004) - The TRANSMED atlas. The Mediterranean region from crust to mantle. Springer, Berlin- Heidelberg.

Cibin U., Spadafora E., Zuffa G.G. & Castellarin A. (2001) - Continental collision history from arenites of episutural basins in the Northern Apennines, Italy. *Geol. Soc. Am. Bull.,* 113: 4-19.

Conti S., Artoni A. & Piola G. (2007) - Seep-carbonates in a thrust-related anticline at the leading edge of an orogenic wedge: the case of the middle-late Miocene Salsomaggiore Ridge (Northern Apennines, Italy). *Sed. Geol.*, 199: 233-251. doi:10.1016/j.sedgeo.2007.01.022.

Conti S. & Fontana D. (2005) - Anatomy of seep-carbonates: ancient examples from the Miocene of the northern Apennines (Italy). *Palaeogeogr. Palaeoclimatol. Palaeoecol.*, 227: 156-175.

Conti S., Fontana D., Lucente C.C. & Pini G. A. (2014) - Relationships between seep-carbonates, mud diapirism and basin geometry in the late Miocene of the northern Apennines of Italy: the Montardone mélange. *Int. J. Earth Sci.,* 103: 281-295.

Conti S., Fontana D., Mecozzi S., Panieri G. & Pini G.A. (2010) - Late Miocene seep-carbonates and fluid migration on top of the Montepetra intrabasinal high (Northern Apennines, Italy): Relations with synsedimentary folding. *Sedim. Geol.*, 231: 41-54.

Conti S. & Gelmini R. (1994) - Miocene-Pliocene tectonic phases and migration of foredeep-thrust belt system in Northern Apennines. *Mem. Soc. Geol. It.,* 48: 261-274.

Conti S., Gelmini R. & Ponzana L. (1993) - Osservazioni preliminari sui calcari a Lucine dell'Appennino Settentrionale. *Atti Soc. Nat. Mat. Modena*, 124: 35-56.

Dickens G.R. (2004) - Hydrocarbon-driven warming. *Nature*, 429: 513-515.

Dickens G. R., O'Neil J. R., Rea D. K. & Owen R. M. (1995) - Dissociation of oceanic methane hydrate as a cause of the carbon isotope excursion at the end of the Paleocene. *Paleoceanography,* 10: 965-971.

Doglioni C., Mongelli F. & Pialli G. (1998) - Boudinage of the Alpine Belt in the Apenninic back-arc. *Mem. Soc. Geol. It.,* 52: 457-468.

Etiope G. (2012) - Methane uncovered. *Nat. Geosci.*, 5: 373-374.

Etiope G., Milkov A.V. & Derbyshire E. (2008) - Did geologic emissions of methane play any role in Quaternary climate change? *Global Planet. Change*, 61: 79-88. doi:10.1016/j.gloplacha.2007.08.008

Fichler C., Henriksen S., Rueslaatten H. & Hovland M. (2005) - North Sea Quaternary morphology from seismic and magnetic data: indications for gas hydrates during glaciation? *Petrol. Geosci.*, 11: 331-337.

Fischer D., Mogollon J. M., Strasser M., Pape T., Bohrmann G., Fekete N., Spiess V. & Kasten S. (2013) - Subduction zone earthquake as potential trigger of submarine hydrocarbon seepage. *Nat. Geosci.*, 6: 647- 651. http://dx.doi.org/10.1038/ngeo1886

Fontana D., Conti S., Grillenzoni C., Mecozzi S., Petruccia F. & Turco E. (2013) - Evidence of climatic control on hydrocarbon seepage in the Miocene of the northern Apennines: the case study of the Vicchio Marls. *Mar. Petr. Geol.*, 40: 90-99. doi: 10.1016/j.marpetgeo.2013.07.014.

Foresi L.M., Bonomo S., Caruso A., Di Stefano A., Di Stefano E., Iaccarino S.M., Lirer F., Mazzei R., Salvatorini G. & Sprovieri R. (2002) - High resolution calcareous plankton biostratigraphy of the Serravallian succession of the Tremiti Islands (Adriatic Sea, Italy). *Riv. It. Paleontol. Strat.*, 108: 257-273.

Greinert J., Bohrmann G. & Suess E. (2001) - Gas hydrate-associated carbonates and methane-venting at Hydrate Ridge: Classification, distribution, and origin of authigenic lithologies. In: Paull C. K. & Dillon W. P. (Eds) - Natural Gas Hydrates: Occurrence, Distribution, and Detection. *Geophys. Monogr.* Ser., vol. 124: 99-113. AGU, Washington, D.C. doi:10.1029/GM124p0099.

Guegen E., Doglioni C. & Fernandez M. (1998) - On the post-25 Ma geodynamic evolution of the western Mediterranean. *Tectonophysics*, 298: 259-269.

Han X., Suess E., Sahling H. & Wallmann K. (2004) - Fluid venting activity on the Costa Rica margin: new results from authigenic carbonates. *Int. J. Earth Sci.* 93: 596-611.

Han X., Suess E., Huang Y., Wu N, Bohrmann G., Su X., Eisenhauer A., Rehder G. & Fang Y. (2008) - Jiulong Methane Reef: Microbial mediation seep-carbonates in the South China Sea. *Mar. Geol.,* 249: 243-256.

Haq B.U., Hardenbol J. & Vail P.R. (1988) - Mesozoic and Cenozoic chronostratigraphy and cycles of sea-level change. In: Wilgus C.K., Hastings B.S., Kendall C.G.St.C, Posamentier H.W., Ross C.A. & Van Wagoner J.C. (Eds) - Sea-level Changes an Integrated Approach. SEPM Spec. Publ., 42: 71, 108.

Hilgen F.J., Abdul Aziz H., Bice D., Iaccarino S., Krijgsman W., Kuiper K., Montanari A., Raffi I., Turco E. & Zachariasse W.J. (2005) - The Global Boundary Stratotype Section and Point (GSSP) of the Tortonian Stage (Upper Miocene) at Monte dei Corvi. *Episodes*, 28: 6-17.

Hilgen F.J., Abdul Aziz H., Krijgsman W., Raffi I. & Turco E. (2003) - Integrated stratigraphy and astronomical tuning of the Serravallian and lower Tortonian at Monte dei Corvi (Middle-Upper Miocene, northern Italy). *Palaeogeogr. Palaeoclimatol. Palaeoecol.*, 199: 229-264. doi.org/10.1016/S0031-0182.

Hilgen F.J., Krijgsman W., Raffi I., Turco E. & Zachariasse W.J. (2000) - Integrated stratigraphy and astronomical calibration of the Serravallian/Tortonian boundary section at Monte Gibliscemi (Sicily Italy). *Mar. Micropaleontol.*, 38: 181-211.

Hill T.M., Kennett J.P., Valentine D.L., Yang Z., Reddy C.M., Nelson R.K., Behl R.J., Robert C. & Beaufort L. (2006) - Climatically driven emissions of hydrocarbons from marine sediments during deglaciation. *PNAS,* 103: 13570-13574.

Hovland M., Judd A.G. & Burke Jr. R.A. (1993) - The global flux of methane from shallow submarine sediments. *Chemosphere*, 26: 559-578.

Hüsing S.K., Hilgen F.J., Abdul Aziz H. & Krijgsman W. (2007) - Completing the Neogene geological time scale between 8.5 and 12.5 Ma. *Earth Planet. Sci. Lett.,* 253: 340-358.

Jørgensen N. O. (1976) - Recent High Magnesian Calcite/Aragonite Cementation of Beach and Submarine Sediments from Denmark. *J. Sedim. Petrol.,* 46: 940-951.

Judd A. & Hovland M. (2007) - Seabed fluid flow. Cambridge University Press, New York, 475 pp.

Kastner M. (2001) - Gas Hydrates in Convergent Margins: Formation, Occurrence, Geochemistry, and Global Significance. In: Paull C.K. & Dillon W.P. (Eds) - Natural Gas Hydrates: Occurrence, Distribution and Detection. *Geoph. Mon.*, 124: 67-86.

Katz M.E., Pak D.K., Dickens G.R. & Miller K.G. (1999) - The source and fate of massive carbon input during the latest Paleocene thermal maximum. *Science*, 286: 1531-1533.

Kennett J., Cannariato K.G., Hendy I.L. & Behl R.J. (2000) - Carbon isotope evidence for methane hydrate instability during Quaternary interstadials. *Science*, 288: 128-133.

Kennett J.P., Cannariato K.G., Hendy I.L. & Behl R.J. (2003) - Role of Methane Hydrates in late Quaternary Climactic Change: The Clathrate Gun Hypothesis. American Geophysical Union: 216 pp.

Kvenvolden K.A. (1993) - Gas Hydrates-Geological perspective and global change. *Rev. Geophys.*, 31: 173-187.

Kvenvolden K.A. & Lorenson T.D. (2001) - The global occurrence of natural gas hydrate. In: Paull C.K. & Dillon W.P. (Eds) - Natural gas hydrates: occurrence, distribution and detection. *AGU Geophys. Monograph*., 124: 3-18.

Kvenvolden K.A. & Rogers B.W. (2005) - Gaia's breath - global methane exhalations. *Mar. Petr. Geol.*, 22: 579-590. doi:10.1016/j.marpetgeo.2004.08.004

Lallemand S.E., Glacon G., Lauriat-Rage A., Fiala-Medioni A., Cadet J.P., Beck C., Sibuet M., Sakai J.T. & Tairo A. (1992) - Seafloor manifestations of fluid seepage at the top of a 2000-metre deep ridge in the eastern Nankai accretionary wedge: Long lived venting and tectonic implications. *Earth Planet. Sci. Lett.*, 109: 333-346.

Laskar J., Robutel P., Joutel F., Gastineau M., Correia A.C.M. & Levrard B. (2004) - A long-term numerical solutin for the insolation quantities of the earth. *Astron. Astrophys.,* 428: 261-285.

Le Pichon X., Kobayashi K. & Kaiko-Nankai Scientific crew (1992) - Fluid venting activity within the eastern Nankai trough accretionary wedge: a summary of the 1989 Kaiko-Nankai results. *Earth Planet. Sci. Lett*., 109: 303-318.

Lirer F., Caruso A., Foresi L.M., Sprovieri M., Bonomo S., Di Stefano A., Di Stefano E., Iaccarino S.M., Salvatorini G., Sprovieri R. & Mazzola S. (2002) - Astrochronological calibration of the upper Serravallian-lower Tortonian sedimentary sequence at Tremiti Islands (Adriatic Sea, Southern Italy). In: Iaccarino S. (Ed.) - Integrated Stratigraphy and Paleoceanography of the Mediterranean Middle Miocene. *Riv. It. Paleontol. Strat.,* 108: 241-256.

Lourens L.J., Hilgen F.J., Laskar J., Shackleton N.J. & Wilson D. (2004) - The Neogene period. In: Gradstein F.M., Ogg J.G. & Smith A.G. (Eds.) - A Geologic Time Scale: 409-440, Cambridge Univ. Press.

Luyendyk B., Kennett J. & Clark J. F. (2005) - Hypothesis for increased atmospheric methane input from hydrocarbon seeps on exposed continental shelves during glacial low sea level. *Mar. Petr. Geol*., 22: 591-596.

Malinverno A. & Ryan W.B.F. (1986) - Extension in the Tyrrhenian sea and shortening in the Apennines as result of arc migration driven by sinking of the lithosphere. *Tectonics,* 5: 227-245.

Maslim M., Mikkelsen N., Vilela C. & Haq B. (1998) - Sea-level-and-gas-hydrate-controlled catastrophic sediment failures of the Amazon fan. *Geology*, 26: 1107-1110.

Maslim M., Owen M., Day S. & Long D. (2004) - Linking continental-slope failures and climate change: testing the clathrate gun hypothesis. *Geology,* 32: 53-56.

Maslim M., Vilela C., Mikkelsen N. & Grootes P. (2005) - Causes of catastrophic sediment failures of the Amazon fan. *Quatern. Sci. Rev.*, 24: 2180-2193.

Mienert J., Vanneste M., Bünz S., Andreassen K., Haflidason H. & Sejrup H.P. (2004) - Ocean warming and gas hydrate stability on the mid-Norwegian margin at the Storrega Slide. *Mar. Petr. Geol.,* 22: 233-244.

Miller K.G., Feigenson J.D., Wrigt J.D. & Clement B.M. (1991a) - Miocene isotope reference section, Deep Sea Drilling Project, Site 608: an evaluation of isotope and biostratigraphic resolution. *Paleoceanography,* 6: 33-52.

Miller K.G., Wright J.D. & Fairbanks R.G. (1991b) - Unlocking the icehouse: Oligocene-Miocene oxygen isotope, eustacy, and margin erosion. *J. Geophys. Res*., 96: 6829-6848.

Milkov A.V. (2004) - Global estimates of hydrate-bound gas in marine sediments: how much is really out there? *Earth-Sci. Rev.*, 66: 183-197.

Monnin E., Indermühle A., Dällenbach J., Flückiger J., Stauffer B., Stocker T.F., Raynaud D. & Barnola J.M. (2001) - Atmospheric CO_2 concentrations over the last glacial termination. *Science*, 291: 112-114.

Mutti E., Ricci Lucchi F. & Roveri M. (2002) - Revisiting turbidites of the Marnoso-arenacea Formation and their basin margin counterparts: problems with classic models. In: Mutti E., Ricci Lucchi F. & Roveri M. (Eds) - Excursion Guidebook 64th EAGE Conference and Exhibition. University of Parma and ENI-AGIP Division, Parma, Italy, 250 pp.

Mutti E., Tinterri R., Benevelli G., Di Biase D. & Cavanna G. (2003) - Deltaic, mixed and turbidite sedimentation of ancient foreland basins. *Mar. Petr. Geol.*, 20: 733-755.

Mutti E., Bernoulli D., Ricci Lucchi F. & Tinterri R. (2009) - Turbidites and turbidity currents from Alpine 'flysch' to the exploration of continental margins. *Sedimentology*, 56: 276-318. doi: 10.1111/j.1365-3091.2008.01019.x

Muzzi Magalhaes P. & Tinterri R. (2010) - Stratigraphy and depositional setting of slurry and contained (reflected) beds in the Marnoso-arenacea Formation (Langhian-Serravallian) Northern Appenines, Italy. *Sedimentology*, 57: 1685-1720.

Nisbet E. (1990) - Climate change and methane. *Nature*, 347: 23.

Obzhirov A., Shakirov R., Salyuk A., Suess E., Biebov N. & Salomatin A. (2004) - Relations between methane venting, geological structure and seismo-tectonics in the Okhotsk Sea. *Geo- Mar. Lett.*, 24: 135-139.

Patacca E., Sartori R. & Scandone P. (1990) - Tyrrhenian Basin and Apenninic Arcs: Kinematics Relations Since Late Tortonian Times. *Mem. Soc. Geol. It.,* 45: 425-451.

Percher I.A., Kukowski N., Ranero C.R. & von Huene R. (2001) - Gas hydrates along the Peru and middle America trench system. In: Paull C.K. & Dillon W.P. (Eds) - Natural gas hydrates: occurrence, distribution and detection. *AGU Geophys. Monograph*., 124: 257-271.

Petit J.R., Jouzel J., Raynaud D., Barkov N.I., Barnola J.M., Basile I., Bender M., Chappellaz J., Davis M., Delaygue G., Delmotte M., Kotlyakov V.M., Legrand M., Lipenkov V.Y., Lorius C., Pépin L., Ritz C., Saltzman E. & Stievenard M. (1999) - Climate and atmospheric history of the past 420,000 years from the Vostok ice core, Antarctica. *Nature*, 399: 429-436.

Piola G. (2003) - Problemi geologico-stratigrafici collegati al tetto della struttura di Salsomaggiore Terme (PR). Unpublished Laurea Thesis, Università degli Studi di Parma, Parma, 123 pp.

Pini G.A. (1999) - Tectosomes and olistostromes in the argille scagliose of Northern Apennines. *Geol. Soc. Am. Spec. Paper* 335, 70 pp.

Posamentier H.W. & Vail P.R. (1988) - Eustatic controls on clastic deposition. II. Sequence and systems tract models. In: Wilgus C.K., Hastings B.S., Kendall C.G.St.C., Posamentier H.W., Ross C.A. & Van Wagoner J.C. (Eds) - Sea Level Changes - An Integrated Approach, SEPM Special Publication, 42: 125-154.

Reed D.L., Silver, E.A., Tagudin T.H., Shipley T.H. & Vrolijk P. (1990) - Relations between mud volcanoes, thrust deformation, slope sedimentation, and gas hydrate, offshore Panama. *Mar. Petr. Geol.*, 7: 44-54.

Ricci Lucchi F. (1975) - Miocene paleogeography and basin analysis in the periadriatic Apennines. In: Squyres C. (Ed.) - Geology of Italy: 5-111. Petroleum exploration society of Libya, Tripoli.

Ricci Lucchi F. (1986) - The Oligocene to Recent foreland basins of the northern Apennines. In: Allen P.A. & Homewood P. (Eds) - Foreland basins: 105-140. Blackwell, Oxford.

Ricci Lucchi F. & Vai G.B. (1994) - A stratigraphic and tectonofacies framework of the "calcari a Lucina" in the Apennine Chain, Italy. *Geo-Mar. Lett.* 14: 210-218.

Royden L., Patacca E. & Scandone P. (1987) - Segmentation and configuration of subducted lithosphere in Italy: an important control on thrust-belt and foredeep-basin evolution. *Geology,* 15: 714-717.

Sassen R., Losh S.L., Cathles III L., Roberts H.H., Whelan J.K., Milkov A.V., Sweet S.T. & De Freitas D.A. (2001) - Massive vein-filling gas hydrates: relation to ongoing gas migration from the deep subsurface in the Gulf of Mexico. *Mar. Petr. Geology*, 18: 551-560.

Schwartz H., Sample J., Weberling K.D., Minisini D. & Moore J.C. (2003) - An ancient linked fluid migration system: cold-seep deposits and sandstone intrusions in the Panoche Hills, California, USA. *Geo-Marine Letters*, 23: 340-350.

Secord R., Gingerich P. D., Lohmann K. C. & MacLeod K. G. (2010) - Continental warming preceding the Palaeocene-Eocene thermal maximum. *Nature*, 467: 955-958. doi:10.1038/nature09441

Shackleton N.J. (1987) - Oxygen isotopes, ice volume and sea level. *Quatern. Sci. Rev.* 6: 183-190.

Shackleton N.J. & Hall M.A. (1997) - The late Miocene stable isotope record, Site 926. In: Shackleton N.J., Curry W.B., Richter C. & Bralower T.J. (Eds) - Proc. ODP, Sci. Results, 154: College Station, TX (Ocean Drilling Program), 367-373. doi:10.2973/odp.proc.sr.154.119.1997.

Shackleton N.J. & Matthews R. K. (1977) - Oxygen isotope stratigraphy of Late Pleistocene coral terraces in Barbados. *Nature,* 268: 618-620.

Sloan jr E.D. (1998) - Physical/chemical properties of gas hydrates and application to world margin stability and climate change. In: Henriet J.P. & Mienert J. (Eds) - Gas hydrates: relevance to world margin stability and climate changes. *Geol. Soc. London Spec. Publ.*, 137: 31-50.

Sluijs A., Brinkhuis H., Schouten S., Bohaty S. M., John C. M., Zachos J. C., Reichart G.-J., Sinninghe Damste J. S., Crouch E. M. & Dickens G. R. (2007) - Environmental precursors to rapid light carbon injection at the Palaeocene/Eocene boundary. *Nature*, 450: 1218-1221. doi:10.1038/nature06400.

Sprovieri R, Bonomo S, Caruso A, Di Stefano A, Di Stefano E., Foresi L.M., Iaccarino S.M., Lirer F., Mazzei R. & Salvatorini G. (2002) - An integrated calcareous plankton biostratigraphic scheme and biochronology for the Mediterranean Middle Miocene. In: Iaccarino S. (Ed.) - Integrated stratigraphy and paleoceanography of the Mediterranean Middle Miocene. *Riv. It. Paleontol. Strat.*, 108: 337-353.

Suess E. (2010) - Marine cold seeps. In: Timmis K.N. (Ed.) - Handbook of hydrocarbon and lipid microbiology. Springer-Verlag Berlin Heidelberg. doi 10.1007/978-3-540-77587-4_12

Suess E. (2011) - Marine gas hydrate research: changing views over the past 25 years. Proceedings of the 7th International Conference on Gas Hydrates (ICGH 2011), Edinburgh, Scotland, United Kingdom, July 17-21, 2011.

Suess E. (2014) - Marine cold seeps and their manifestations: geological control, biogeochemical criteria and environmental conditions. *Int. J. Earth Sci. (Geol. Rundsch.)* 103: 1889-1916. doi: 10.1007/s00531-014-1010-0.

Suess E. & Haeckel M. (2010) - Gashydrate im meeresboden. *Geogr. Rundsh.* 5: 22-29.

Suess E., Bohrmann G., Von Huene R., Linke P., Wallmann K., Lammers S., Sahling H., Winckler G., Lutz R.A. & Orange D. (1998) - Fluid venting in the eastern Aleutian subduction zone. *J. Geophys. Res.*, 103(B2): 2597-2614.

Suess E., Torres M.E., Bohrmann G., Collier R.W., Greinert J., Linke P., Rehder G., Trehu A., Wallmann K., Winckler G. & Zuleger E. (1999) - Gas hydrate destabilization: enhanced dewatering, benthic material turnover and large methane plumes at the Cascadia convergent margin. *Earth Planet. Sci. Lett.*, 170: 1-15.

Taviani M. (2001) - Fluid venting and associated processes. In: Vai G.B. & Martini I.P. (Eds) - Anatomy of an Orogen: the Apennines and adjacent Mediterranean basins: 351-366. Kluwer Acad. Publ., London.

Taviani M. (2014) - Marine chemosynthesis in the Mediterranean Sea. In: Goffredo S. & Dubinsky Z. (Eds) - The Mediterranean Sea: Its history and present challenges: 69-83. Springer, Dordrecht.

Teichert B.M.A., Eisenhauer A., Bohrmann G., Haase-Schramm A., Bock B. & Linke P. (2003) - U/Th systematics and ages of authigenic carbonates from Hydrate Ridge, Cascadia Margin: recorders of fluid flow variations. *Geochim. Cosmochim. Acta*, 67(20): 3845-3857. doi:10.1016/S0016-7037(03)00128-5.

Tinterri R. & Muzzi Magalhaes P. (2011) - Sedimentary structural control on foredeep turbidites: an example from Miocene Marnoso-arenacea Formation, Northern Apennines, Italy. *Mar. Petrol. Geol.*, 28: 629-657.

Tréhu A.M., Long P.E., Torres M.E., Bohrmann G., Rack F.R. Collett T.S., Goldberg D.S., Milkov A.V., Riedel M., Schultheiss P., Bangs N.L., Barr S.R., Borowski W.S., Claypool G.E., Delwiche M.E., Dickens G.R., Gracia E., Guerin G., Holland M., Johnson J.E. Lee Y.-J., Liu C.-S., Su, X., Teichert B., Tomaru H., Vanneste M., Watanabe M. & Weinberger J.L. (2004) - Three-dimensional distribution of gas hydrate beneath southern Hydrate Ridge: constraints from ODP Leg 204. *Earth Planet. Sci. Lett.*. 222: 845-862.

Tréhu A.M, Ruppel C., Holland M., Dickens G. R., Torres M. E., Collett T. S., Goldberg D., Riedel M. & Schultheiss P. (2006) - Gas hydrates in marine sediments. *Oceanography*, 19: 124-142.

Tréhu A.M., Torres M.E., Moore G.F., Suess E. & Bohrmann G. (1999) - Temporal and spatial evolution of gas hydrate-bearing accretionary ridge on the Oregon continental margin. *Geology*, 27: 939-942.

Turco E., Hilgen F.J., Lourens L.J., Shackleton N.J. & Zachariasse W.J. (2001) - Punctuated evolution of global climate cooling during the late middle to early late Miocene: high-resolution planktonic foraminiferal and oxygen isotope records from the Mediterranean. *Paleoceanography*, 16: 405-423.

Von Rad U., Berner U., Delisle G., Doose-Rolinski H., Fechner N., Linke P., Luckge A., Roeser H.A., Schmalijohann R., Wiedicke M. & SONNE 122/130 Scientific Parties (2000) - Gas and fluid venting at the Makran accretionary wedge off Pakistan. *Geo-Mar. Lett.*, 20: 10-19.

Warrick R.A., Barrow E.M. & Wigley T.M.L. (2009) - Climate and sea level change: observations, projections and implications. Cambrige University Press, Cambridge, 424 pp.

Weinberger J.L. & Brown K.M. (2006) - Fracture networks and hydrate distribution at Hydrate Ridge, Oregon. *Earth Planet. Sci. Lett.*, 245: 123-136.

Wiedicke M., Sahling H., Delisle G., Faber E., Neben S., Beiersdorf H., Marchig V., Weiss, W., Von Mirbach N. & Afiat A. (2002) - Characteristics of an active vent in the fore-arc basin of the Sunda Arc, Indonesia. *Mar. geol.*, 184: 121-141.

Wright J.D. & Miller K.G. (1992) - Miocene stable isotope stratigraphy, Site 747, Kerguelen Plateau. *Proc. Oc. Drill. Program. Sci. Res*. 120: 855-866.

Wuebbles D.J. & Hayhoe K. (2002) - Atmospheric methane and global change. *Earth-Sci. Rev.*, 57: 177-210.

Zanzucchi G. (Ed.) (2000) - Note illustrative della Carta Geologica d'Italia 1:50.000, F. 198 Bardi. Carta Geologica d'Italia 1:50.000, Roma, 75 pp.